JOURNAL OF GEOPHYSICAL RESEARCH, VOL. 95, NO. B6, PAGES 8543–8567, JUNE 10, 1990

Tectonic History and New Isochron Chart of the South Pacific

CATHERINE L. MAYES

Department of Geological Sciences and Institute for Geophysics, University of Texas at Austin

LAWRENCE A. LAWVER AND DAVID T. SANDWELL[1]

Institute for Geophysics, University of Texas at Austin

We have developed an internally consistent isochron chart and a tectonic history of the South Pacific using a combination of new satellite altimeter data and shipboard magnetic and bathymetric data. Highly accurate, vertical deflection profiles (1-2 μrad), derived from 22 repeat cycles of Geosat altimetry, reveal subtle lineations in the gravity field associated with the South Pacific fracture zones. These fracture zone lineations are correlated with sparse shipboard bathymetric identifications of fracture zones and thus can be used to determine paleospreading directions in uncharted areas. The high density of Geosat altimeter profiles reveals previously unknown details in paleospreading directions on all of the major plates. Magnetic anomaly identifications and magnetic lineation interpretations from published sources were combined with these fracture zone lineations to produce a tectonic fabric map. The tectonic fabric was then used to derive new poles of rotation for 12 selected times in the Late Cretaceous and Cenozoic. From our reconstructions, we estimated the former location of the spreading centers in order to derive a new set of isochrons (interpreted lines of equal age on the ocean floor). We believe that the use of new Geosat altimeter data in combination with a multi-plate reconstruction has led to an improvement in our understanding of South Pacific tectonics.

INTRODUCTION

The South Pacific covers 75 x 10^6 km^2 and represents one-sixth of the world's oceans. Our study area (75° of latitude by 110° of longitude) includes four major plates (Pacific, Antarctic, Cocos, and Nazca). It is bordered to the east by Central and South America; to the south by Antarctica; to the west by the Macquarie Ridge, New Zealand, and the Tonga-Kermadec Trench system; and to the north by the equator (Figure 1 and Plate 1). Whereas past studies have focused on one or two of the spreading centers in the South Pacific, we have attempted to summarize the tectonic history of the entire region from the Early Cretaceous to the present in an internally consistent model and to identify any problems that might result from the combination of individual models incorporated into this project.

The South Pacific is so vast and remote that ship track coverage of bathymetric and magnetic data is highly variable and frequently sparse. In some parts of the South Pacific, for example, along the East Pacific Rise north of 22°S, there are over 50 ship tracks per million square kilometers, but even these tracks are not uniformly spaced. In the south central part of the region, however, there are only 6-26 nonuniformly spaced tracks per million square kilometers. We have been able to greatly improve the data coverage of the South Pacific by using satellite altimeter measurements of the marine gravity field collected by Geosat [*Cheney et al.*, 1987]. To further improve the accuracy, resolution, and coverage of the Geosat profiles, we have averaged 22 repeat cycles from the first year of the exact repeat mission. In this data set, there are 36 uniformly spaced tracks per million square kilometer near the equator increasing to more than 70 tracks per million square kilometer at high latitudes. The average track spacing of the Geosat data is 82 km at the equator, and decreases to less than 40 km at high latitudes [*McConathy and Kilgus*, 1987].

Geosat measures the topography of the sea surface, which is nearly an equipotential surface of the Earth's gravity field called the geoid. Variations in sea surface topography reflect mass deficits and surpluses associated with seafloor topography. Features such as seamounts, troughs, and fracture zones produce characteristic signatures in the sea surface topography with amplitudes well above the noise level of the satellite altimeter. For example, an oceanic fracture zone produces a step in the sea surface that can be traced across many Geosat altimeter profiles. These fracture zone lineations correspond to tectonic flow lines and thus record the direction of relative plate motion. Subtle changes in the trends of the flow lines reflect changes in the stage poles of relative motion between the plates. Paleospreading directions (from Geosat data) combined with spreading rate information (from magnetic anomaly identifications) allow us to derive an internally consistent model of plate motions.

To derive the tectonic model, we first compiled and summarized previous magnetic anomaly and bathymetric studies of the South Pacific. We then identified fracture zone lineations on vertical deflection profile maps derived from Geosat altimeter data. We combined published magnetic anomaly identifications with the fracture zone lineations to construct a new tectonic chart. The digitized data were separated into tectonic elements (plates) and displayed on an interactive graphics terminal where each plate could be rotated about its pole. Using this interactive terminal, a set of self-consistent stage poles were determined for all of the plate pairs at each of 12 times. The tectonic reconstruction of the South Pacific at a particular time is the sum of the stage poles from the present to that time. From the past

[1]Now at Geologic Research Division, Scripps Institution of Oceanography, La Jolla, California.

Paper number 89JB02731.
0148-0227/90/89JB-02731$05.00

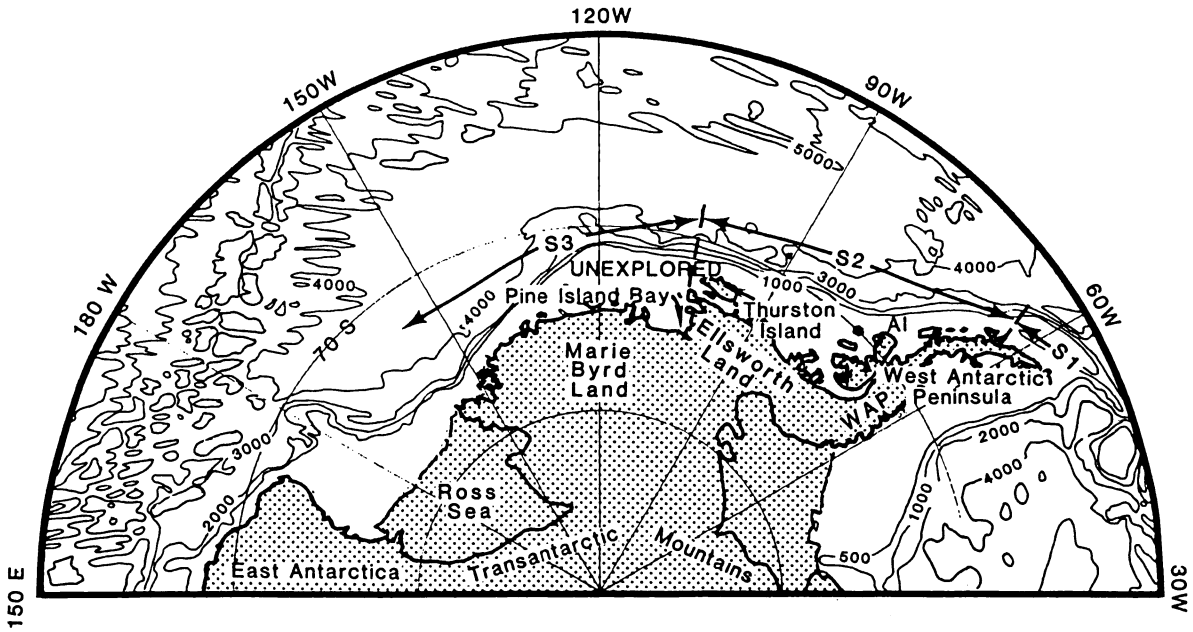

Fig. 1. Bathymetry (in meters) in a polar stereographic projection. S1, segment 1, the section of the West Antarctic margin that may still be undergoing subduction, although subduction probably ceased about 4 m.y. ago. S2, segment 2, the section of the West Antarctic margin that underwent subduction but subduction ceased anywhere from 20 to 50 m.y. ago [Barker, 1982]. S3, segment 3, the Marie Byrd Land margin that has only been a divergent margin.

positions of the spreading centers at each time, we derived an isochron chart of the entire South Pacific.

Our study has implications for several fields: global plate motion circuits, the evolution of the Antarctic and Andean margins, plate motions in New Zealand, and ocean circulation. This work can be used to predict the age of unexplored or uninterpreted parts of the South Pacific. A regional tectonic study of the South Pacific can be used to constrain certain geologic problems along its margins. For instance, consideration of Antarctic-Pacific motion, combined with data concerning Antarctic-Australia motion, can help define the motion between the northern and southern parts of New Zealand and the history of the opening of the Ross Sea between East and West Antarctica. Such consideration also has implications for the history of the Antarctic margin.

TECTONIC SETTING

The South Pacific (Figure 1 and Plate 1) is composed of four major plates: the Pacific, the Antarctic, the Nazca and the Cocos (Plate 2). The Pacific plate is the largest of all the plates. It comprises virtually all of the ocean floor in the Pacific north of the equator and two-thirds of the Pacific ocean floor south of the equator and has been in existence since at least the Jurassic [*Larson*, 1976]. The oldest magnetic anomaly on the Pacific plate near the equator is in the Phoenix lineations and is identified as Late Jurassic (M25, 156 Ma [*Kent and Gradstein*, 1985]). The Pacific plate is separated from the Cocos and Nazca plates by the East Pacific Rise [*Menard*, 1960, 1966; *Sclater et al.*, 1971; *Herron*, 1972; *Anderson and Sclater*, 1972; *Handschumacher*, 1976; *Klitgord and Mammerickx*, 1982; *Pardo-Casas and Molnar*, 1987; *Rosa and Molnar*, 1988], and from the Antarctic plate by the Pacific-Antarctic Rise [*Pitman et al.*, 1968; *Molnar et al.*, 1975; *Weissel and Hayes*, 1977; *Christoffel and Falconer*, 1972; *Cande et al.*, 1982; *Stock and Molnar*, 1987]. For the Late Cretaceous to the present, identifiable marine magnetic anomalies and fracture zone trends define the spreading history of the Pacific relatively well. The older crust, created during the Cretaceous Magnetic Quiet Period (118 to 84 Ma [*Palmer*, 1983]), has very smooth bathymetry and little magnetic signature. This older crust is located just to the east of the Tonga trench (Plate 2), and its tectonic history can only be surmised.

Some of the major features on the Pacific plate, other than the spreading ridges that define the major plate boundaries, are the seamount chains and plateaus (Figure 1 and Plate 1). In the northern half of the South Pacific, the Marquesas, Tuamotu, and Austral islands appear to be located on a bathymetric high on the GEBCO 5.11 bathymetry chart [*Mammerickx and Smith*, 1984*b*]. Farther to the west, the Manihiki Plateau rises 2500 m above the surrounding seafloor and is composed of oceanic material [*Lanphere and Dalrymple*, 1976]. In the southwest Pacific, the Louisville Ridge is a nearly unbroken chain of seamounts extending from the Tonga-Kermadec Trench to about 46°S, 157°W [*Watts et al.*, 1988; *Lonsdale*, 1988].

The Antarctic plate is the second-largest constituent of the South Pacific seafloor (Figure 1 and Plate 2) and its tectonic history is complex. There is evidence for major ridge jumps and substantial ridge reorientations [e.g., *Cande et al.*, 1982; *Barker*, 1982]. Significant parts of the oceanic crust of the Antarctic plate are covered with ice year round, so the marine magnetic record for the Antarctic plate is incomplete. The oldest remaining oceanic part of the Antarctic plate in the South Pacific is probably Late Cretaceous in age [*Barker*, 1982; *Cande et al.*, 1982]. The Antarctic plate is separated from the Nazca plate by an active spreading center, the Chile Rise [*Cande et al.*, 1982; *Cande and Leslie*, 1986].

The continental Antarctic plate can be divided into two major pieces, East Antarctica and West Antarctica. West Antarctica is composed of several blocks [*Dalziel and Elliot*, 1982; *Grunow*

et al., 1987]: the West Antarctic Peninsula block, the Ellsworth-Whitmore Mountains block, the Haag Nunataks block, the Thurston Island-Eights Coast block, and Marie Byrd Land. We treat the West Antarctic blocks as one entity from the Late Cretaceous to the present based on the paleomagnetic results of *Grunow et al.* [1987]. We use the Transantarctic Mountain Front as the division between East and West Antarctica (I. W. D. Dalziel, personal communication, 1988).

The Cocos and Nazca plates are remnants of the older Farallon plate (Plates 1 and 2). These two plates are now slowly spreading apart along the nearly equatorial, east-west trending Galapagos Spreading Center [*Hey*, 1977; *Klitgord and Lonsdale*, 1978; *Klitgord and Mammerickx*, 1982]. Magnetic anomalies created at the old Pacific-Farallon spreading center are preserved on the Nazca plate close to the South American margin (Plate 2). To the south, between the East Pacific Rise (EPR) and the South American margin (5°-17°S and 95°-97°W), the Galapagos Rise forms a linear topographic high which was interpreted as a failed spreading center by *Anderson and Sclater* [1972] and by *Mammerickx et al.* [1980]. Near the equator it is difficult to identify magnetic anomalies formed at the EPR because it is spreading in an east-west direction and the extruded basalt is only weakly magnetized in the vertical direction. Therefore the age and spreading history of crust on parts of the Nazca plate remain ill-defined, and for the same reasons, the ages of much of the Cocos plate also remain unknown.

The Pacific-Antarctic Rise boundary contains a number of very large offset fracture zones which are apparent on bathymetric charts (Figure 1 and Plate 1), even with the very limited coverage in this region. The Eltanin Fracture Zone system (Plate 2) is the most remarkable of these features. This system consists of two major fracture zones, the Heezen and the Tharp fracture zones, along with several fracture zones with smaller offsets. The Heezen Fracture Zone offsets the ridge by 350 km; the Tharp Fracture Zone has a larger offset of 650 km. Immediately to the north and south of the Eltanin system, the Menard and Udintsev fracture zones also have large offsets on the Pacific-Antarctic Rise. The Chile Rise is offset by two major fracture zones: the Valdivia Fracture Zone at 41°S and the Guafo Fracture Zone at 45°S (Plate 2). The western third of the Antarctic plate boundary with the Nazca plate is a large-offset fracture zone called the Chile Fracture Zone. The length of the Chile Fracture Zone is approximately 800 km. The fracture zones along the EPR and the Galapagos Spreading Center are relatively small-offset fracture zones, with most offsets less than 150 km, as opposed to the 300 km offset of the Udintsev Fracture Zone along the Pacific-Antarctic Ridge.

Two active microplates have been identified in the South Pacific. Between 22° and 27°S on the EPR (Plate 2), a new ridge has developed to the east of the old EPR [*Handschumacher et al.*, 1981]. The EPR appears to be in the process of jumping from the old ridge, Oeste (Spanish for west), 400 km to the east to the new ridge named Este (Spanish for east). This ridge jump defines the Easter microplate which appears to have been in existence for 3.2 my. The Juan Fernandez microplate between 31° and 35°S is defined by bathymetry and earthquakes at the Pacific-Nazca-Antarctic triple junction [*Anderson-Fontana et al.*, 1986]. At the Juan Fernandez microplate the EPR again appears to be jumping from a west ridge to an east ridge, with spreading having been initiated on the east ridge about 3 Ma (Plate 2). There are at least two older major ridge jumps in the South Pacific region which will be discussed later.

The South Pacific region is bordered by a combination of trenches, transform faults, and passive margins. The plate boundary between the Pacific and Australian plates is convergent or transpressional along different parts of the plate boundary [e.g., *Kamp*, 1986]. This plate boundary trends north along the Macquarie Ridge and through New Zealand along the Alpine Fault (Figure 1 and Plate 1).

Bordering the Pacific crust to the west is the Tonga-Kermadec Trench system. There have been subduction zones to the west of the Pacific plate spreading regimes since at least the Cretaceous. The Lord Howe Rise (Plate 1), a submerged block of rhyolite [*Burns et al.*, 1973] of continental crustal thickness, is possibly related to subduction along this margin. The Lord Howe Rise can be reconstructed to Australia by closing the Tasman Sea [*Hayes and Ringis*, 1973; *Weissel and Hayes*, 1977]. Back-arc spreading which formed the rest of the marginal basins of the South Pacific is probably responsible for the reorientation of the trench to its current position [*Karig*, 1970]. The Vitiaz-Solomon-New Britain Trench system forms the remaining boundary of the Pacific plate in our study area.

Along the eastern margin of the Pacific Ocean basin, Cocos, Nazca, and Antarctic crust is subducted beneath Central and South America at the Middle America and Peru-Chile trenches. We estimate that the Peru-Chile Trench has consumed at least 6000 km of Farallon, Nazca, and Cocos plates since Chron 34. The Shackleton Transform fault, which extends from the southern tip of South America to the northern tip of the West Antarctic Peninsula, forms the boundary between the recently deceased Antarctic-Drake spreading regime and the extinct spreading system of the western Scotia Sea. The Pacific margin of West Antarctica can be split into three segments (Figure 1). From the Shackleton Fracture Zone to the Hero Fracture Zone (Plate 2), the margin is characterized as a recently convergent margin which resulted from subduction of the Drake plate beneath the West Antarctic Peninsula [*Barker*, 1982]. Extension and volcanism is still active in the Bransfield Straits (Figure 1 and Plate 1), but arc-related volcanism ceased almost 50 m.y. ago [*Barker*, 1982]. The segment of the margin between the Hero Fracture Zone and Pine Island Bay was once a subduction margin [*Barker*, 1982]. There have been a series of ridge-trench collisions at different times along this margin which resulted in the cessation of the differential motion between the oceanic crust immediately to the north and West Antarctica [*Herron and Tucholke*, 1976; *Barker*, 1982]. The ridge-trench collisions resulted in the incorporation of the oceanic crust as part of the Antarctic plate. The third segment of the West Antarctic margin, adjacent to Marie Byrd Land, lies between Pine Island Bay and the Ross Sea. This segment is the conjugate passive margin to the Campbell Plateau and the Chatham Rise (offshore New Zealand) to the north [*Molnar et al.*, 1975; *Crook and Belbin*, 1978; *Stock and Molnar*, 1987; *Grindley and Davey*, 1982].

DATA

Compilation of Shipboard Magnetic and Bathymetric Data

The shipboard data used in our study consist of previously identified magnetic anomalies, interpreted magnetic lineations and identified fracture zone crossings (Plate 2). We have not reidentified any magnetic anomalies. Therefore there may be small inconsistencies in our model because different authors picked different parts of the magnetic anomalies (i.e., peaks, troughs, or inflection points). In our compilation of shipboard

data, we have used the following identifications of lineation pattern and fracture zones: *Klitgord and Mammerickx* [1982] for the northern East Pacific Rise and the Galapagos Spreading Center; *Mammerickx et al.* [1980] for the Galapagos Rise; *Handschumacher* [1976] for the southern East Pacific Rise, with some identifications from *Herron* [1972]; *Pardo-Casas and Molnar* [1987] for the older mid-Tertiary anomalies along the old Pacific-Farallon spreading center; *Cande et al.* [1982] for the oldest anomalies on the Pacific-Farallon spreading center; and *Cande et al.* [1982] with *Cande and Leslie* [1986] for the Chile Rise. For anomalies along the Pacific-Antarctic Rise, we have used identifications and lineations from *Molnar et al.* [1975], *Weissel and Hayes* [1977], *Cande et al.* [1982], *Christoffel and Falconer* [1972], and *Stock and Molnar* [1987], while along the Antarctic margin, we used the identifications of *Herron and Tucholke* [1976] and *Barker* [1982]. Except for the small regions of seafloor older than Chron 34 just south of the Campbell Plateau and to the north and west of the anomaly 34 identifications of *Cande et al.* [1982], all the crust in the South Pacific is younger than Chron 34.

Ship track coverage in the South Pacific region is highly variable because the region is so immense and because many parts of the area are far from most normal shiping lanes. There are many large areas between fracture zones with no magnetic picks or lineations. Also, many of the published fracture zone lineations are not based on sufficient exploration to show the true trends and complexities of the real fracture zones in the South Pacific. Consequently, we have used satellite altimetry data to provide us with more detail, in order to define relative plate motion.

Vertical Deflection Fabric Chart (Geosat)

Sandwell and Schubert [1982], *Sailor and Okal* [1983], *Haxby* [1987], *Cande et al.* [1988], *Craig and Sandwell* [1988], and *Okal and Cazenave* [1985] used satellite altimetry data to locate seafloor features and trace tectonic lineations. All of these papers use data from the Seasat (Sea Satellite) altimeter. Data from the Geosat (Geodesy Satellite) altimeter have a higher degree of accuracy than equivalent Seasat data. Geosat data can be processed to a precision of 3.5 cm for significant wave heights of 2 m [*McConathy and Kilgus*, 1987; *MacArthur et al.*, 1987],

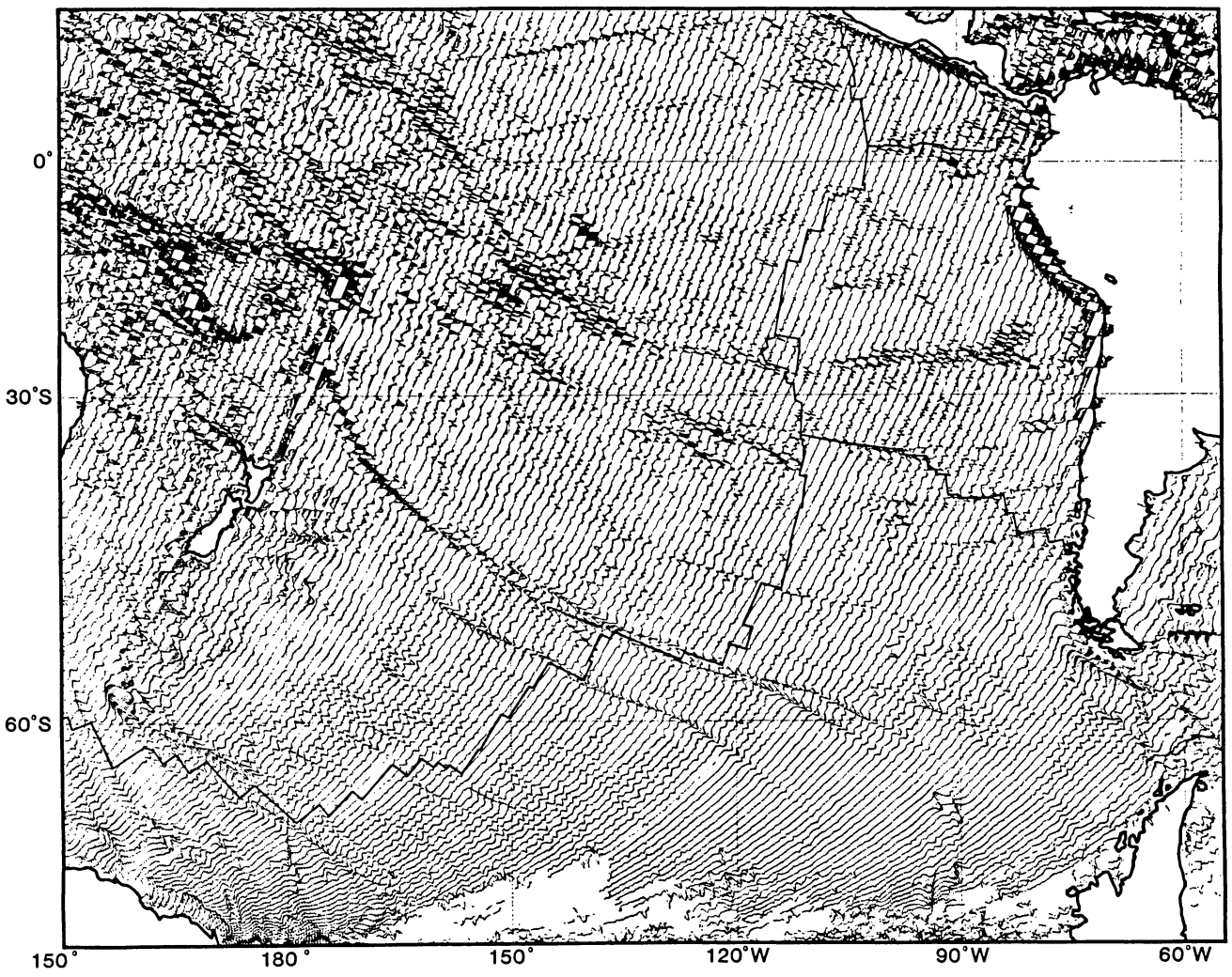

Fig. 2*a*. Deflection of the vertical, plotted perpendicular to track for descending passes, in the South Pacific. Present-day spreading centers are drawn with a light solid line. Small dots mark earthquake locations (bulletin of the International Seismological Centre).

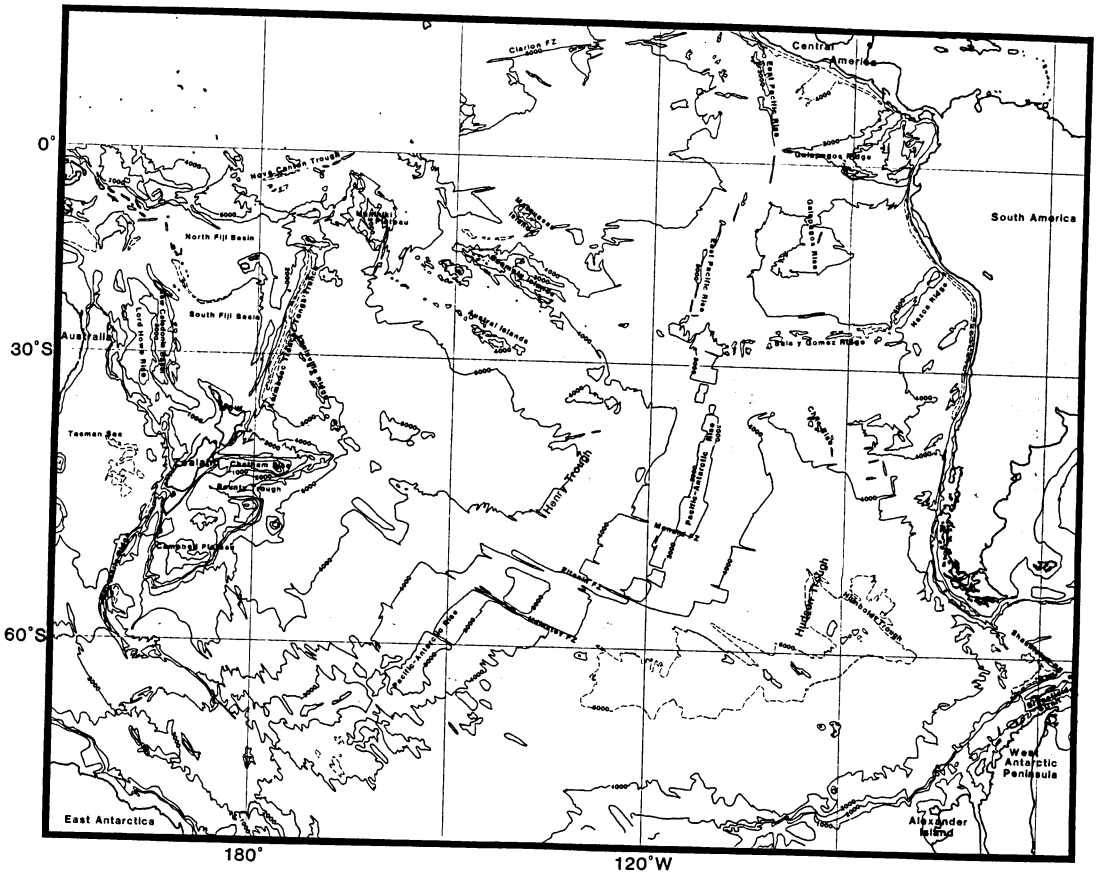

Plate 1. Bathymetry (in meters) and major features of the South Pacific region (from mini-GEBCO, version 5.0).

120°W 90°W 60°W

descending passes, in the South Pacific. Present-day
nake locations (bulletin of the International Seismological

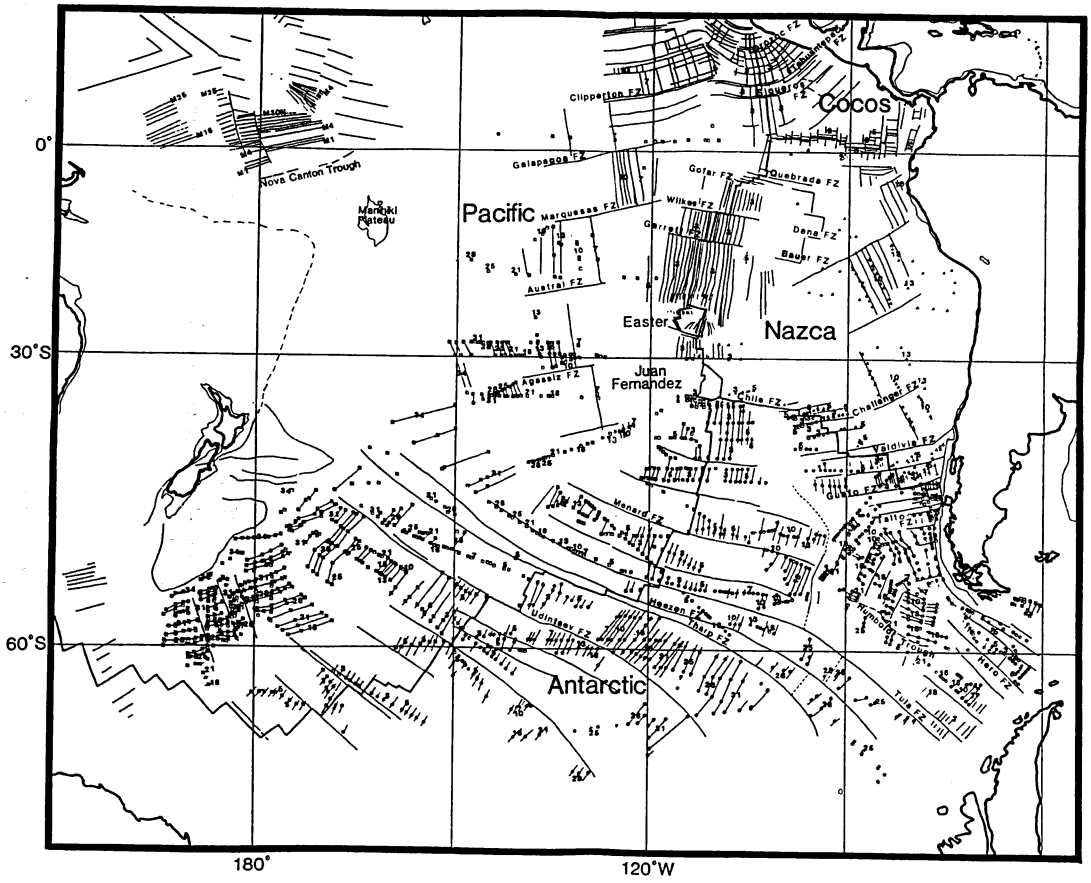

Plate 2. Compilation of magnetic picks and lineations and fracture zones for the South Pacific. Sources include *Klitgord and Mammericks* [1982], *Herron* [1972], *Handschumacher* [1976], *Pardo-Casas and Molnar* [1987], *Mammericks et al.* [1980], *Handschumacher et al.* [1981], *Cande et al.* [1982], *Larson* [1976], *Herron and Tucholke* [1976], *Barker* [1983], *Molnar et al.* [1975], *Weissel and Hayes* [1977], *Christoffel and Falconer* [1972].

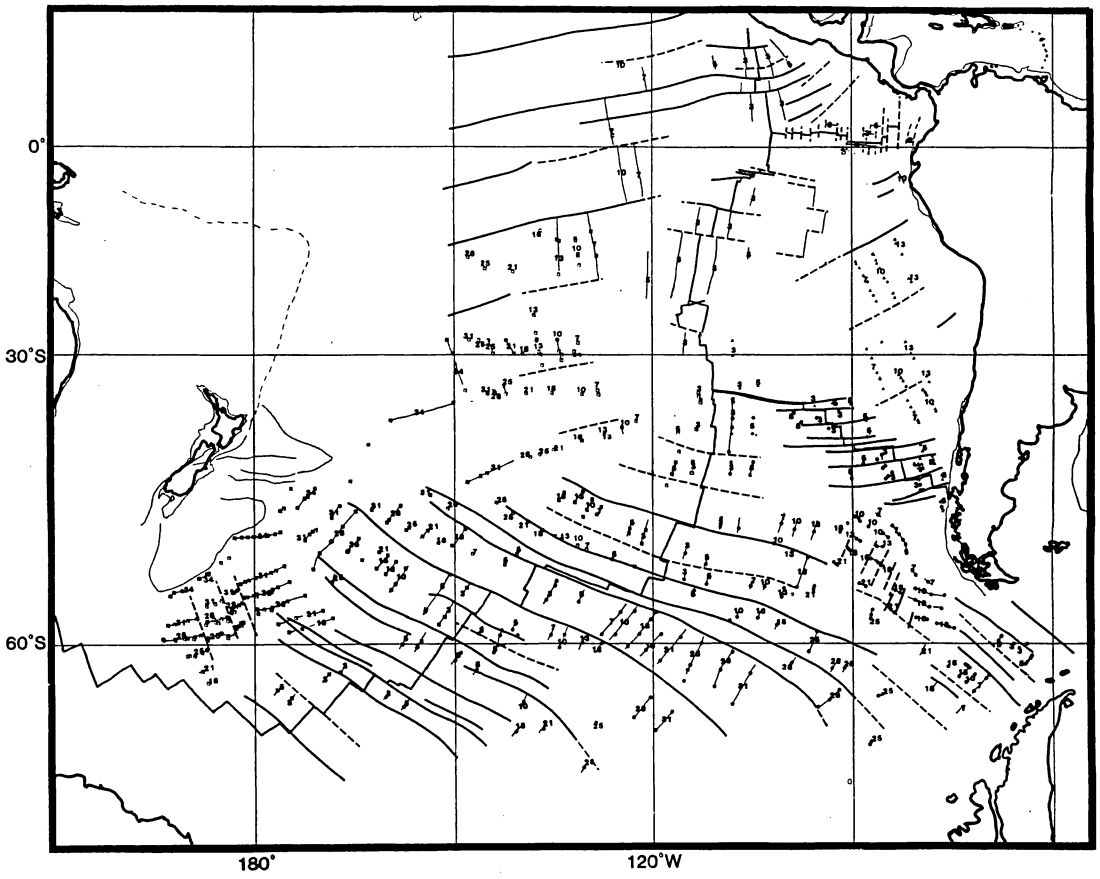

Plate 3. Generalized tectonic fabric map of the South Pacific. Magnetic picks and lineations from published sources are combined with the tectonic fabric derived from the deflection of the vertical (solid lines). Where there are no good vertical deflection lineations, i.e., on the fast spreading Pacific-Nazca plate boundary and on the small-offset fracture zones on the Galapagos Spreading Center, bathymetric identifications (dashed lines) have been included.

better by a factor of 2.9 than the 10-cm accuracy of Seasat data for wave heights less than 20 m [*Tapley et al.*, 1982]. The Geosat began its unclassified Exact Repeat Mission (ERM) in October 1987 and was in operation during the Austral summer of 1987-1988, unlike the Seasat satellite which lasted only 3 months before it failed in October 1978. During the Austral summer, the sea ice around Antarctica is at a minimum and Geosat recorded a geoid signal in high southern latitudes, which is noteworthy because of the sparse ship track coverage in the area [*Sandwell and McAdoo*, 1988]. Since Geosat was placed in the unclassified 17-day ERM, the equatorial track spacing has been 164 km [*McConathy and Kilgus*, 1987]. We averaged 22 Geosat altimeter repeat cycles to improve the precision of the data and to enhance data coverage of the South Pacific region.

The Geosat data consist of satellite passes in two directions: ascending (those travelling from southeast to northwest) and descending (those traveling from northeast to southwest) (Figure 2). Since the main interest of our study is the identification of tectonic flow lines, we combine the ascending and descending passes to make our interpretations. The flow lines are generated by features which have relatively short wavelengths in the geoid, so the slope of the geoid is used rather than the geoid itself. The first derivative of the geoid, or the slope, is called the deflection of the vertical or vertical deflection. It is plotted perpendicular to the ground tracks (Figure 2). The data were filtered by a Gaussian filter to remove wavelengths shorter than 19.8 km. The longest wavelengths (greater than 4000 km) were also removed using the spherical harmonic coefficients of the PGS-54 gravity model [*Marsh and Martin*, 1982]. The data were filtered for two reasons: the shorter wavelengths are filtered out because they are below the threshold of noise; the longer wavelengths are related to deep-seated gravity anomalies and thermal convection and therefore are presumed not to be a reflection of the bathymetry.

Seamounts and trenches were picked at the zero crossing between peaks and troughs on plots of the deflection of the vertical (Figure 3). It is difficult to correlate the lineations in the satellite altimeter data with the bathymetric locations of fracture zones, because the gravity signatures of fracture zones vary with spreading rate [*Shaw and Cande*, 1987]. We use the satellite altimetry data to predict the spreading direction by determining tectonic flow lines which parallel the fracture zones, since we cannot locate the fracture zones themselves. Flow lines indicate the direction of relative plate motion, and we can use them just as we use fracture zone identifications to constrain tectonic reconstructions.

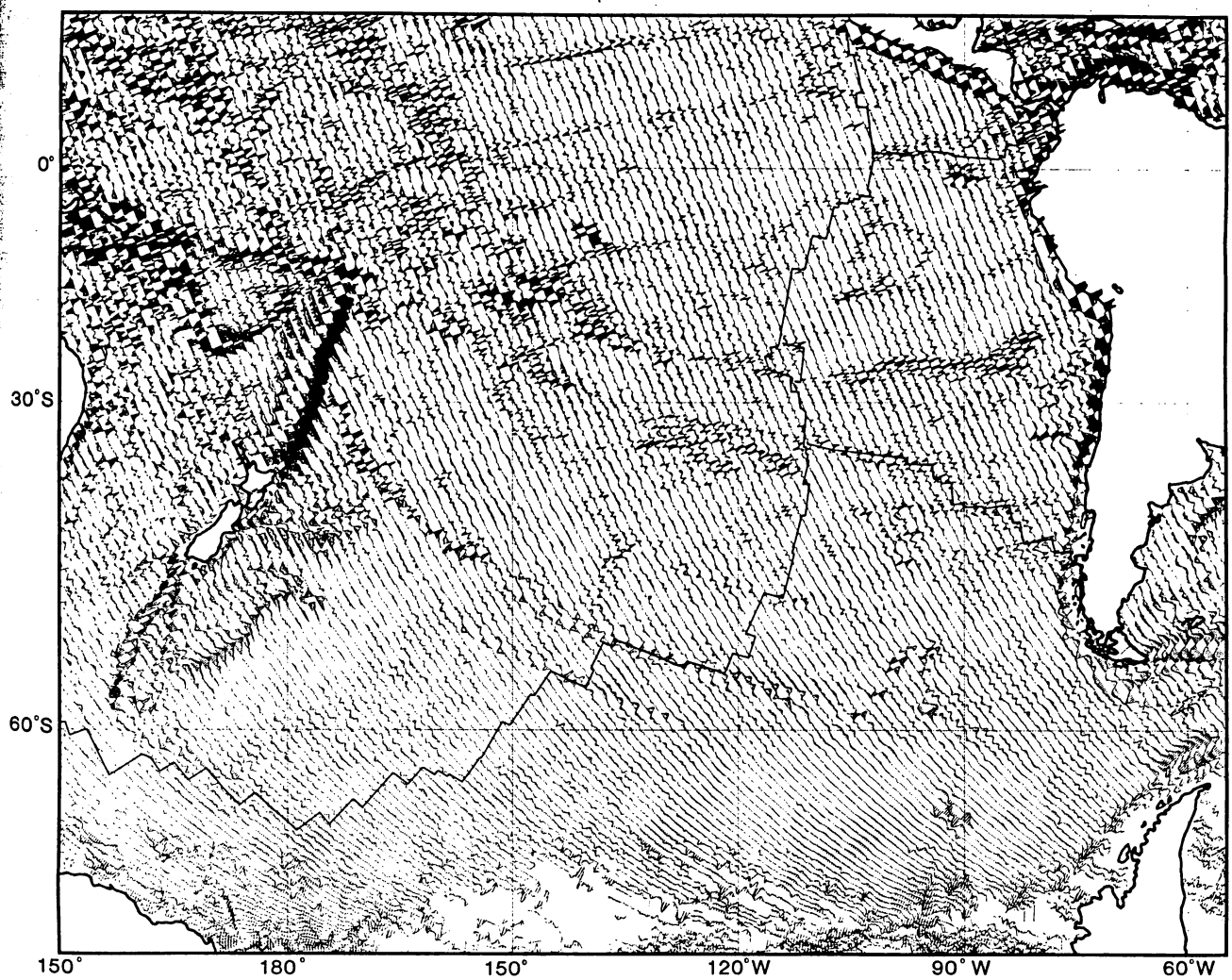

Fig. 2*b*. Deflection of the vertical, plotted perpendicular to track for ascending passes, in the South Pacific.

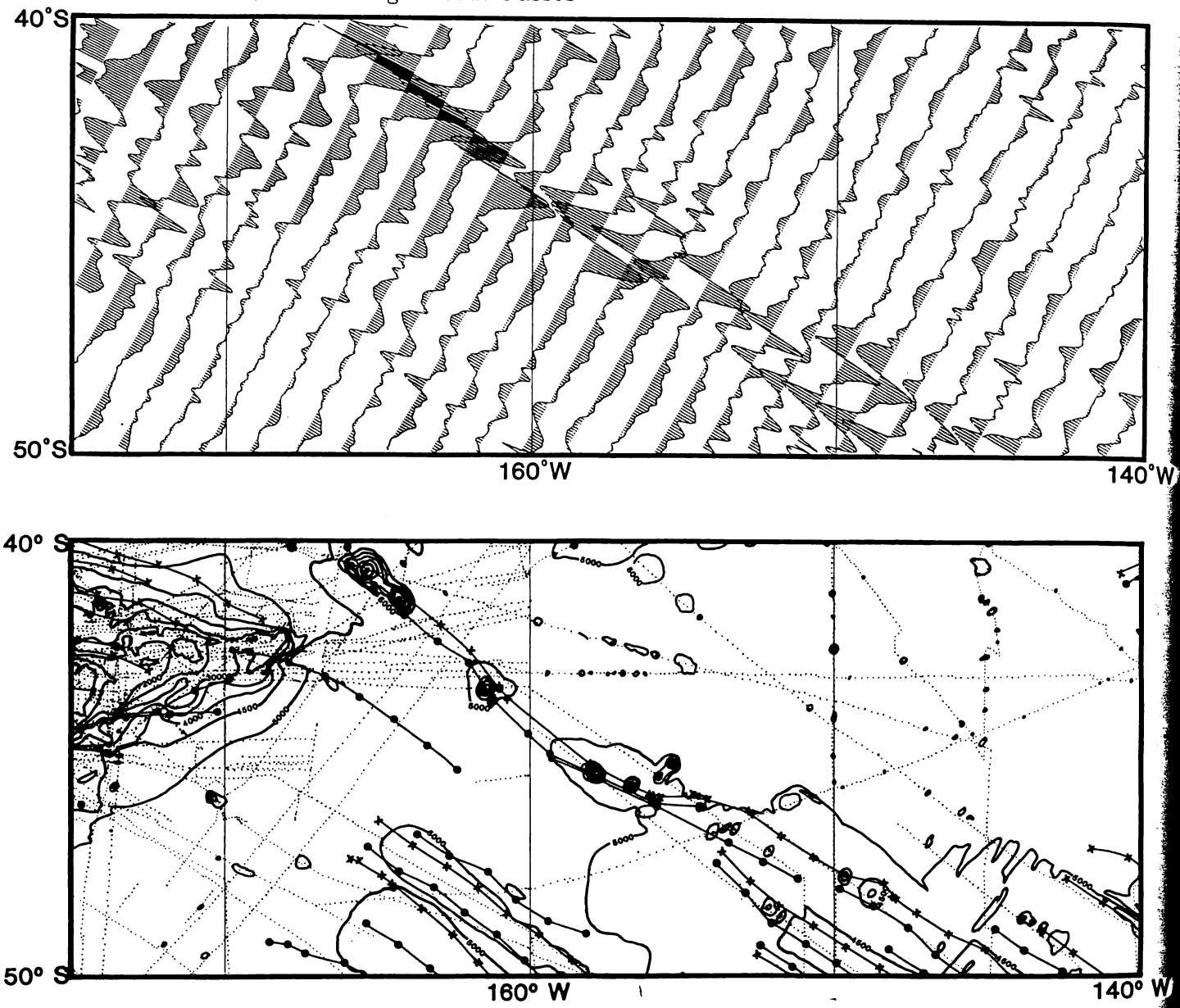

Fig. 5a. Comparison of vertical deflection and bathymetry over the northern portion of the Eltanin fracture zone system. Bathymetry from GEBCO chart 5.15 [*Mammerickx et al.*, 1984] in 500 m intervals. Dotted lines are ship tracks. Picks from the vertical deflection tracks are indicated as either dots (same as circles in Figure 4) or crosses (same as crosses in Figure 4). There is a close correspondence between the bathymetry and the vertical deflection lineations.

step up in topography on one side of the active transform from older crust to younger crust and a step down from younger to older on the other (Figure 6). We feel that use of the vertical deflection lineations, in conjunction with the bathymetric identifications, to constrain the spreading direction is a better method for calculating poles of rotation than the use of bathymetric identifications alone because the vertical deflection lineations have in many cases a much denser and generally more uniform sample interval than lineations determined on the basis of bathymetric identifications alone.

METHODS FOR CALCULATING POLES OF RECONSTRUCTION

After compilation of the data, we utilized an Evans and Sutherland PS300 interactive graphics system to reconstruct plate locations through time [*Scotese et al.*, 1988]. We assigned the digitized data to individual tectonic elements, or plates. Each tectonic element can be displayed and can be independently rotated about any pole of rotation relative to any of the other plates displayed on the surface of a virtual sphere. Plate rotations were determined by the best visual fit of the data. We then used a computer program which utilized the hierarchical tectonic analysis technique on an interactive graphics terminal [*Ross and Scotese*, 1988] to reconstruct the plates that we identified by their relative positions in the past. The reconstructions were done beginning with the present and working backward in time. We used the younger reconstructions since they are better constrained as starting points for older reconstructions.

The relative poles of rotation between plate pairs were calculated in stages corresponding to time intervals between

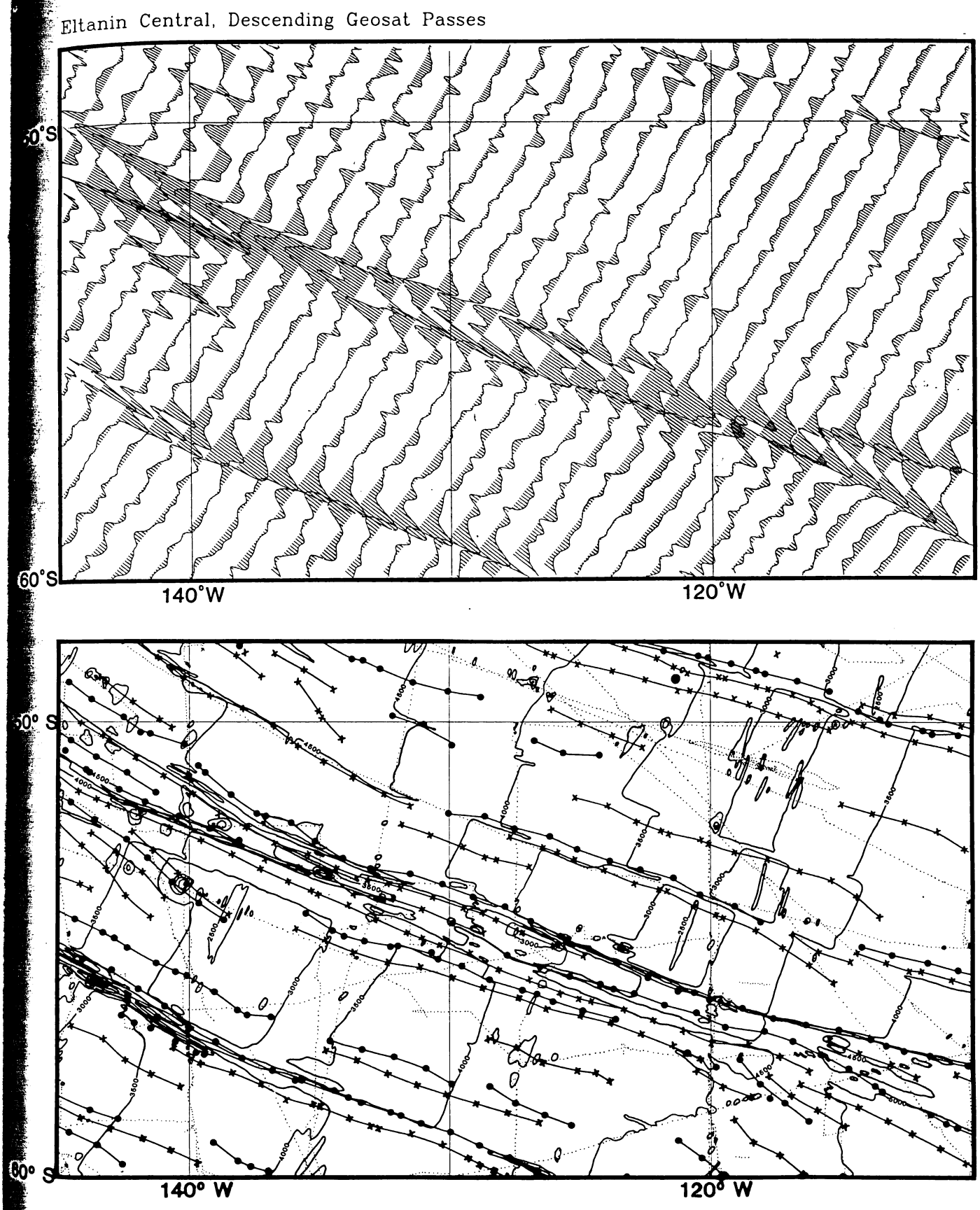

Fig. 5*b*. Comparison of deflection of the vertical and bathymetry over the central portion of the Eltanin fracture zone system.

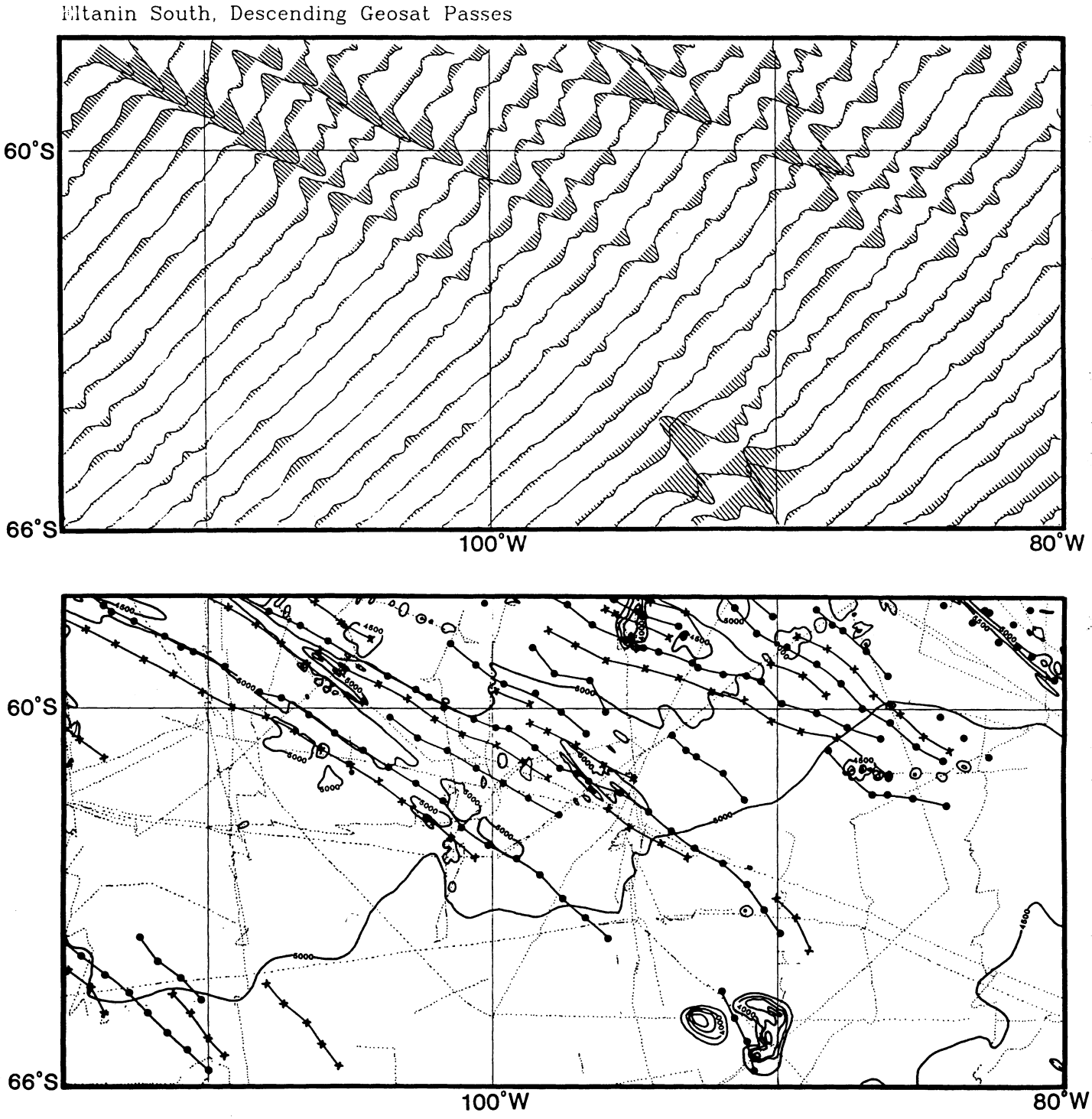

Fig. 5c. Comparison of deflection of the vertical and bathymetry over the southern portion of the Eltanin fracture zone system.

significant magnetic anomalies. The sum of a series of stage poles corresponds to the finite pole over the interval spanned by the stages. For example, to calculate the finite pole for Chron 10 for Pacific-Antarctic relative motion, we first reconstructed the Antarctic plate to its Chron 7 position, relative to a Pacific plate fixed in present-day coordinates (stage 1). We then moved the Pacific plate relative to the reconstructed Antarctic plate, and matched the anomaly 10 identifications, lineations and flowlines on each plate (stage 2). For each stage of the reconstruction, the tectonic fabric lineations were used to determine spreading direction while magnetic anomaly identifications provided most of the timing information as well as some of the directional information. The finite pole of rotation for Chron 10 is the sum of the two stages.

In the cases where ages were identified on only one side of a spreading center (i.e., when one plate has been subducted, is covered with ice, or has no magnetic anomaly identifications), a different procedure was used to calculate poles of rotation. In

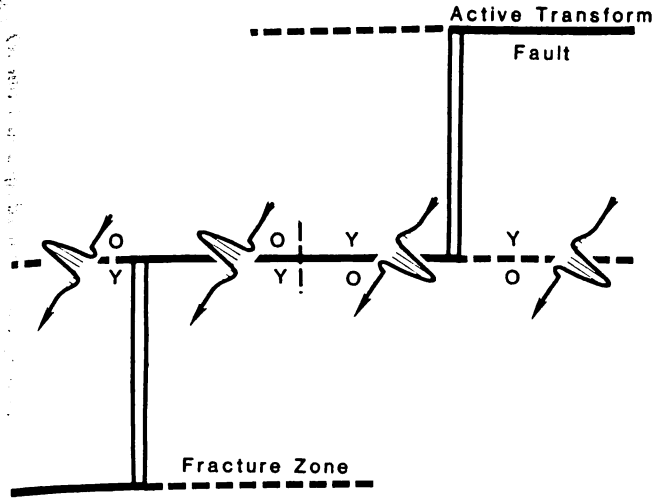

Fig. 6. Deflection of the vertical over a fracture zone/transform fault in the vicinity of a ridge. Y, side of the transform or fracture zone on which crust is younger. O, side of transform fault or fracture zone where crust is older. A lineation drawn on a line of peaks on one side of the active ridge is matched with the lineation from a line of troughs on the other side of the ridge. The ridge position can be estimated by identifying the change in polarity along a fracture zone lineation.

these cases, we rotated younger picks onto older anomalies using a stage pole which has small circles parallel to the direction of the tectonic flowlines. Assuming symmetric spreading, this rotation angle approximates the half angle for the stage pole of relative motion between the two plates. By doubling the angle and adding this stage pole to the finite pole for the younger anomaly, we calculated the finite pole of rotation for these anomalies. We were forced to use this method for Pacific-Farallon spreading older than Chron 13 and for Pacific-Antarctic spreading older than Chron 18.

To test the accuracy and self-consistency of the poles, we calculated the full spreading rates, directions and the stage poles for Pacific-Antarctic (Bellingshausen), Pacific-Antarctic (Weddellia), and Pacific-Nazca (Farallon) plate pairs. Spreading rates and directions were plotted against time to check for consistency and smoothness of changes in orientation and rate (Figure 7). We plotted small circles for the entire length of the ridges in 1° intervals and compared the small circle trends with the trends of our tectonic fabric lineations. We then used the small circles and the matched anomaly picks and lineations, with additional constraints from ridges drawn for younger reconstructions, to draw the spreading center for a particular reconstruction. These spreading centers are assigned to their respective plates, and we use them as isochrons.

We derived finite poles of reconstruction for 12 times in the past. The times of our reconstructions were selected because they have a relatively large number of magnetic anomaly identifications associated with them. We used the Decade of North American Geology (DNAG) time scale [*Berggren et al.*, 1985; *Kent and Gradstein*, 1985] to assign ages to our reconstructions (Table 1). The finite poles of rotation used are given in Table 2. The finite poles for anomalies 5, 13, 25, and 31, for Pacific-Antarctic (Bellingshausen) fall within the uncertainty regions calculated by *Stock and Molnar* [1982] and J. Stock (personal communication, 1988). We make the distinction between an "anomaly" and the time of a particular anomaly by using the term "anomaly" to refer to the magnetic anomaly identification and "chron" to refer to the time of the anomaly, using the convention of *Harland et al.* [1982] and *Klitgord and Schouten* [1986].

TECTONIC HISTORY: A SUMMARY

The seafloor spreading that produced the present-day southwest Pacific, began at around Chron 34 (84.0 Ma). Prior to that time, seafloor spreading occurred along the Pacific-Farallon boundary to the east and the Pacific-Aluk plate boundary to the north (Figure 8). The Aluk and Pacific plates were subducted beneath New Zealand, the Chatham Rise, and the Antarctic margin to the east of Pine Island Bay at that time. New Zealand, the Chatham Rise, and the Campbell Plateau were all part of Gondwanaland, with the Chatham Rise and Campbell Plateau contiguous to Marie Byrd Land [*Grindley and Davey*, 1982]. The Chatham Rise and the Campbell Plateau rifted away from Marie Byrd Land just prior to Chron 34 (84.0 Ma), based on the reidentification of *Christoffel and Falconer*'s [1972] "anomaly 36" to anomaly 34

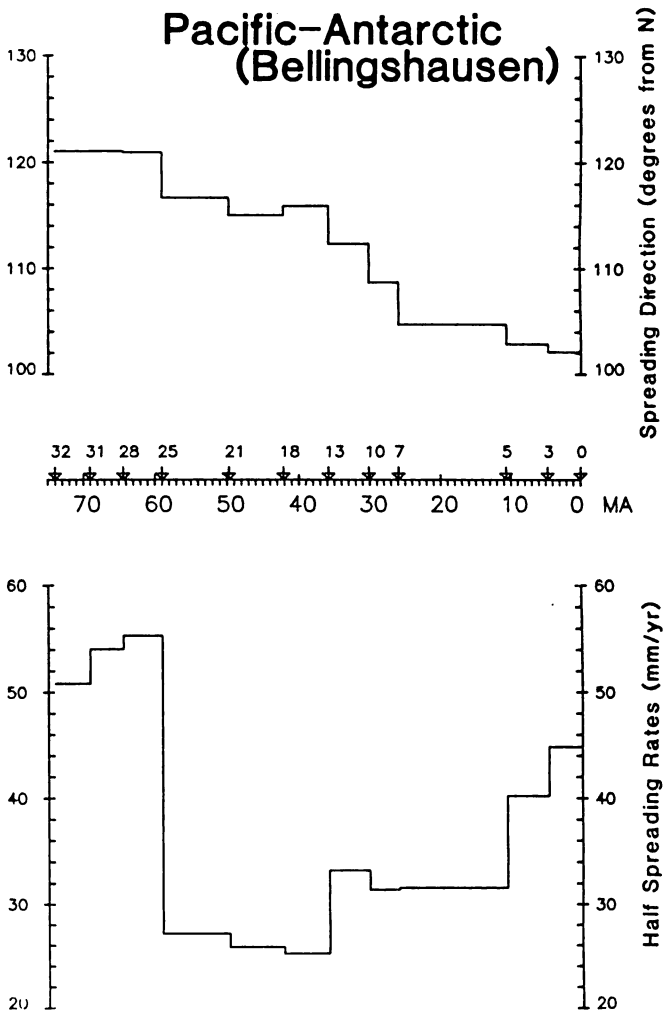

Fig. 7*a*. Spreading azimuths and half rates calculated using the finite poles of rotation of the Antarctic (Bellingshausen)/Pacific plate pair at 42°S, 85°W on the northern segment of the Pacific-Antarctic Rise. Azimuths shown are directions of spreading on the Pacific plate. Azimuths are nearly east-west at present and gradually increase to 115° east.

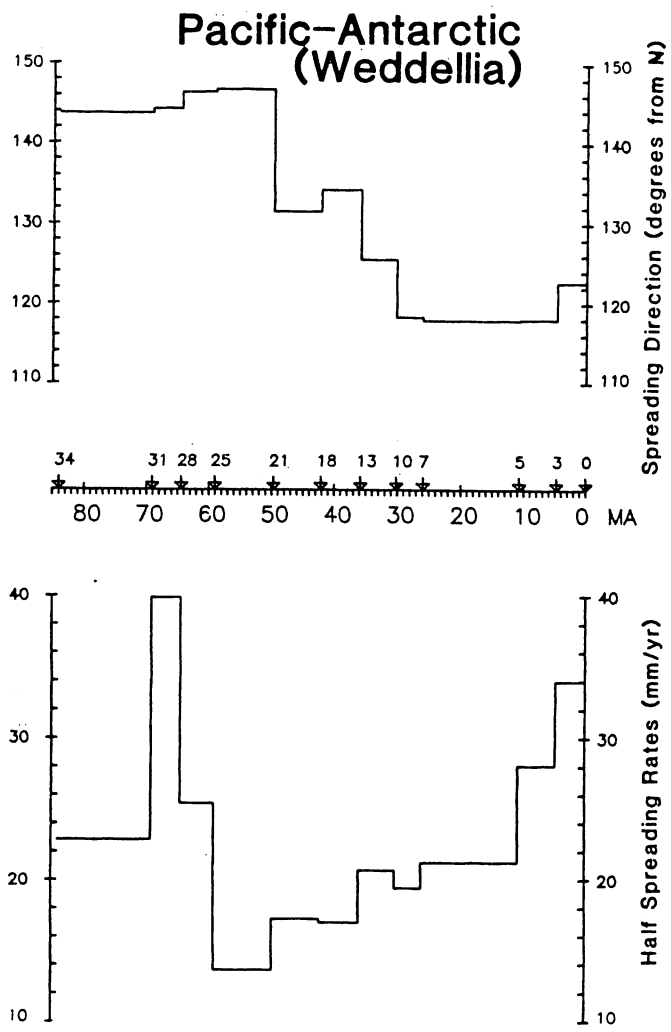

Fig. 7b. Spreading rates and azimuths for the Antarctic (Weddellia)/Pacific plate pair at 65°S, 170°W on the southern portion of the Pacific-Antarctic Rise. Prior to Chron 21 (49.6 Ma), the Pacific and West Antarctica were opening about a different pole than the Pacific-Bellingshausen farther north. Azimuths shown are on the Pacific plate. Azimuths along the Pacific/Marie Byrd Land spreading center are around S20°E. As the Pacific-Antarctic Rise starts spreading along one pole, the azimuths decrease to S50°E. Spreading rates show a corresponding change.

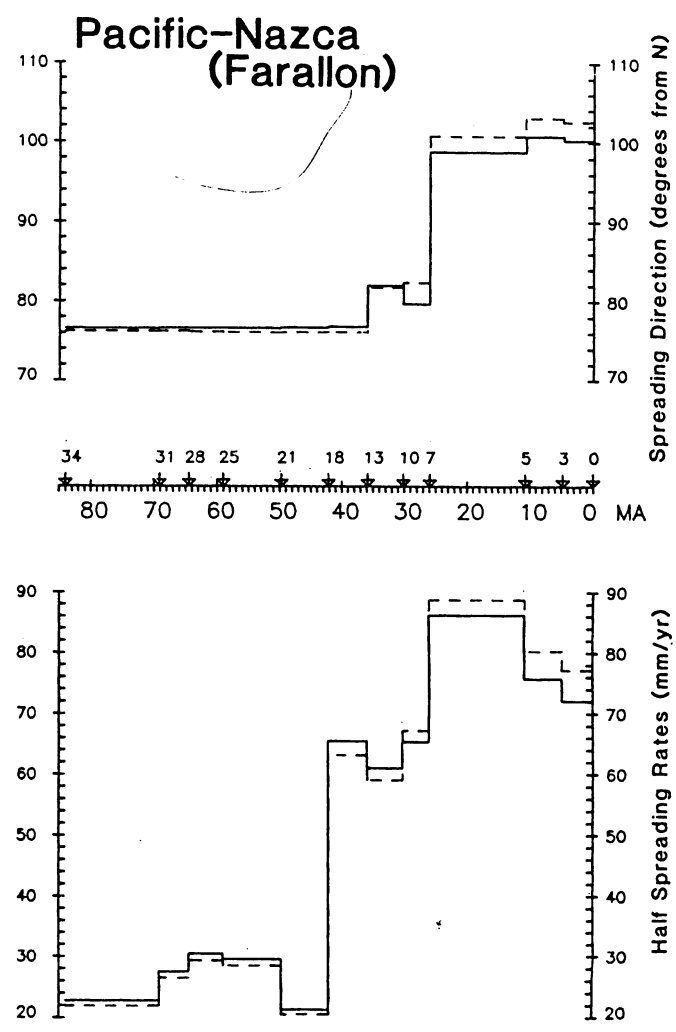

Fig 7c. Spreading azimuths and rates along the Pacific/Nazca (Farallon) boundary at 5°S, 105°W (solid lines) and 46°S, 112°W (dashed lines). Azimuths shown are on the Pacific plate. The spreading rate increases to 120 mm/yr at Chron 18 (42.0 Ma), but the azimuth does not begin to change until Chron 13. The major change in azimuth occurs between Chrons 7 and 5, at which time the spreading rate increases to 160 mm/yr.

TABLE 1. Ages Assigned to Reconstructions and Magnetic Anomalies

Anomaly	Time, Ma
0	0.0
3	4.7
5	10.6
7	25.8
10	30.0
13	35.7
18	42.0
21	49.6
25	58.9
28	64.3
31	69.0
34	84.0

Based on *Berggren et al.* [1985].

just south of our interpretation of the continental margin of the Campbell Plateau (J. Stock, personal communication, 1988). The opening of the Bounty Trough between the Campbell Plateau and the Chatham Rise probably happened just prior to the opening between the Campbell Plateau and Marie Byrd Land. *Stock and Molnar* [1987] suggest that a triple junction was active at 52°S and 173°W between the Pacific, Antarctic and Bellingshausen plates.

Prior to Chron 29 (65.8 Ma), a triple junction developed between the Bellingshausen, Pacific and Aluk plates [*Cande et al.*, 1982]. As this triple junction migrated eastward, dual spreading centers were left behind. During the period between Chron 29 and Chron 25, the dual spreading centers extended eastward in the southeast Pacific (Figure 9). Between the Heezen and Tharp fracture zones, the two spreading centers, Pacific-Bellingshausen and Pacific-Aluk, began to spread apart prior to Chron 29. Just prior to Chron 28, the two spreading centers propagated eastward between the Tharp and Tula fracture zones.

TABLE 2. Finite Poles of Rotation (full spreading rates)

Anomaly	Time	Latitude	Longitude	Angle	Reference
			South America to Africa		
0	0.0	0.00	0.00	0.00	Present
6	20.0	59.00	-35.00	7.70	Lawver et al. [1985]
13	35.5	59.00	-35.00	13.70	Lawver et al. [1985]
28	64.0	63.00	-36.00	24.30	Lawver et al. [1985]
34	84.0	63.00	-36.00	33.80	Lawver et al. [1985]
M0	116.0	55.10	-35.70	50.90	Lawver et al. [1985]
			Australia to Antarctica		
0	0.0	0.00	0.00	0.00	
5	10.5	13.30	37.70	-6.62	Royer and Sandwell [1989]
6	20.5	14.50	32.80	-11.98	Royer and Sandwell [1989]
13	35.5	13.40	32.70	-20.40	Royer and Sandwell [1989]
18	42.0	16.60	29.90	-23.62	Royer and Sandwell [1989]
20	46.2	14.80	30.90	-24.33	Royer and Sandwell [1989]
24	56.1	13.80	30.50	-25.32	Royer and Sandwell [1989]
31	68.5	9.00	33.50	-25.83	Royer and Sandwell [1989]
33	80.2	6.20	35.00	-26.37	Royer and Sandwell [1989]
34	84.0	5.20	5.70	-26.85	Royer and Sandwell [1989]
FIT	96.0	1.00	38.00	-28.30	Royer and Sandwell [1989]
			East Antarctica to Africa		
0	0.0	0.00	0.00	0.00	
2	1.9	18.55	-36.41	0.33	Royer and Sandwell [1989]
3A	5.9	9.45	-41.72	0.82	Royer and Sandwell [1989]
5	10.6	8.50	-51.80	1.44	Royer and Sandwell [1989]
6	20.5	13.40	-55.10	2.79	Royer and Sandwell [1989]
8	27.7	13.60	-51.80	4.02	Patriat [1983]
15	37.7	8.73	-36.52	5.93	Royer and Sandwell [1989]
20	46.2	11.40	-43.70	7.81	Royer and Sandwell [1989]
21	49.6	10.30	-42.90	8.77	Royer and Sandwell [1989]
24	56.1	6.70	-40.60	9.97	Royer and Sandwell [1989]
26	60.8	3.80	-39.70	10.63	Royer and Sandwell [1989]
28o	64.3	0.60	-39.20	11.32	Royer and Sandwell [1989]
29	66.2	-0.40	-39.40	11.59	Royer and Sandwell [1989]
31o	68.4	1.10	-41.60	11.84	Royer and Sandwell [1989]
32	71.7	-1.80	-41.40	13.47	Royer and Sandwell [1989]
33	80.2	-4.70	-39.70	16.04	Royer and Sandwell [1989]
34	84.0	-2.00	-39.20	17.85	Royer and Sandwell [1989]
			Weddellia to East Antarctica		
0	0.0	0.00	0.00	0.00	
33	82.0	0.00	0.00	0.00	
34	84.0	14.82	-20.98	-5.90	This Paper
FIT	90.0	70.26	76.70	-10.48	This Paper
			North New Zealand (Lord Howe Rise) to Australia		
0	0.0	0.00	0.00	0.00	
25	60.0	0.00	0.00	0.00	Weissel and Hayes [1977]
26	65.0	-1.50	138.50	-2.55	Weissel and Hayes [1977]
29	69.0	-5.50	140.50	-6.60	Weissel and Hayes [1977]
32	75.0	-11.40	141.50	-12.75	Weissel and Hayes [1977]
33	82.0	-14.00	142.00	-19.00	Weissel and Hayes [1977]
FIT	90.0	-14.00	142.00	-23.00	Weissel and Hayes [1977]
			Chatham Rise to Pacific		
0	0.0	0.00	0.00	0.00	
32	74.0	0.00	0.00	0.00	
34	84.0	0.00	0.00	0.00	
FIT	90.0	-31.65	143.87	-4.21	Crook and Belbin [1978]

TABLE 2. (continued)

Anomaly	Time	Latitude	Longitude	Angle	Reference
			Bellingshausen Plate to Pacific		
0	0.0	0.00	0.00	0.00	
25	58.9	71.81	-60.67	-39.39	This Paper
28	64.3	70.77	-58.37	-45.52	This Paper
31	69.0	70.31	-56.34	-50.92	This Paper
			Pacific to Marie Byrd Land (Weddellia)		
0	0.0	0.00	0.00	0.00	
3	4.7	66.20	-83.50	4.13	This Paper
5	10.6	70.44	-78.84	9.12	This Paper
7	25.8	73.13	-72.44	19.52	This Paper
10	30.0	73.73	-69.54	22.52	This Paper
13	35.7	73.67	-65.98	26.68	This Paper
18	42.0	72.78	-64.61	29.89	This Paper
21	49.6	72.09	-63.44	33.93	This Paper
25	58.9	70.32	-63.45	36.77	This Paper
28	64.3	68.69	-63.47	39.88	This Paper
31	69.0	67.12	-63.02	44.53	This Paper
34	84.0	64.94	-62.49	53.09	This Paper
FIT	90.0	64.03	-56.96	57.65	This Paper
			Nazca to Pacific		
0	0.00	0.00	0.00	0.00	
3	4.7	58.86	-89.43	-6.60	This Paper
5	10.6	60.13	-89.76	-15.18	This Paper
7	25.8	65.41	-92.00	-39.35	This Paper
10	30.0	66.20	-98.41	-44.05	This Paper
13	35.7	69.04	-104.34	-49.63	This Paper
18	42.0	71.68	-113.62	-56.17	This Paper
21	49.6	72.45	-117.31	-58.80	This Paper
25	58.9	73.47	-123.51	-63.31	This Paper
28	64.3	73.94	-127.15	-66.04	This Paper
31	69.0	74.24	-129.95	-68.20	This Paper
34	84.0	74.81	-137.06	-73.96	This Paper
			Cocos to Pacific		
0	0.0	0.00	0.00	0.00	
3	4.7	31.62	-106.80	-10.64	This Paper
5	10.6	47.13	-106.64	18.57	This Paper

At approximately 50 Ma, the spreading centers in the South Pacific underwent a major change in configuration (Figure 10). Spreading along the oceanic Antarctic-Bellingshausen plate boundary ceased, and the Pacific-Antarctic spreading center south of the triple junction and the Pacific-Bellingshausen spreading center to the north of it became one Pacific-Antarctic spreading center opening with respect to a common pole [*Stock and Molnar*, 1987]. Farther to the east, the remainder of the Aluk-Pacific ridge jumped northward, almost instantaneously from the Tula Fracture Zone [*Cande et al.*, 1982] to just west of the Menard Fracture Zone (Figure 10, fracture zones identified on Plate 2) and became the eastward extension of the Pacific-Antarctic Ridge. When this happened, a piece of the Pacific plate created at the Pacific-Aluk spreading center was transferred to the Antarctic plate and the ANTA-ALUK-PACF (or BEL-ALUK-PACF) triple junction became the ANTA-PCF-FARA triple junction. Anomalies 21-27 created on the Pacific plate now appear on the Antarctic plate south of the Humboldt Fracture Zone, whereas the northward aging anomalies 28-34 that were formed at the Pacific-Aluk boundary are still on the Pacific plate [*Cande et al.*, 1982]. The scars left from the new rift that extended the Pacific-Antarctic ridge to the Farallon plate are the Henry Trough on the Pacific plate and the Hudson Trough on the Antarctic plate. Both the Henry Trough and the Hudson Trough can be clearly seen in the vertical deflection lineations (Figure 4).

Prior to the major ridge reorganization at Chron 21, the Farallon plate had undergone a change in relative motion. The magnetic lineations of *Cande et al.* [1982] indicate that the Farallon plate began to rift away from the Pacific-Aluk spreading segment along the Humboldt Trough just prior to anomaly 23 (54.0 Ma). The spreading center, which is now the Chile Rise, had an orientation parallel to the Humboldt Trough, with a spreading direction perpendicular to the Humboldt Trough. The lineations created at this ridge are now preserved on the Antarctic plate to the north of the Humboldt Trough.

The plate boundaries were fairly stable in the South Pacific region between anomaly 18 and anomaly 7 (42.0-25.8 Ma). However, during this time period, the Antarctic-Farallon spreading center rotated from an orientation of N60°W to an orientation of N20°W as new crust was accreted to the Antarctic plate. The

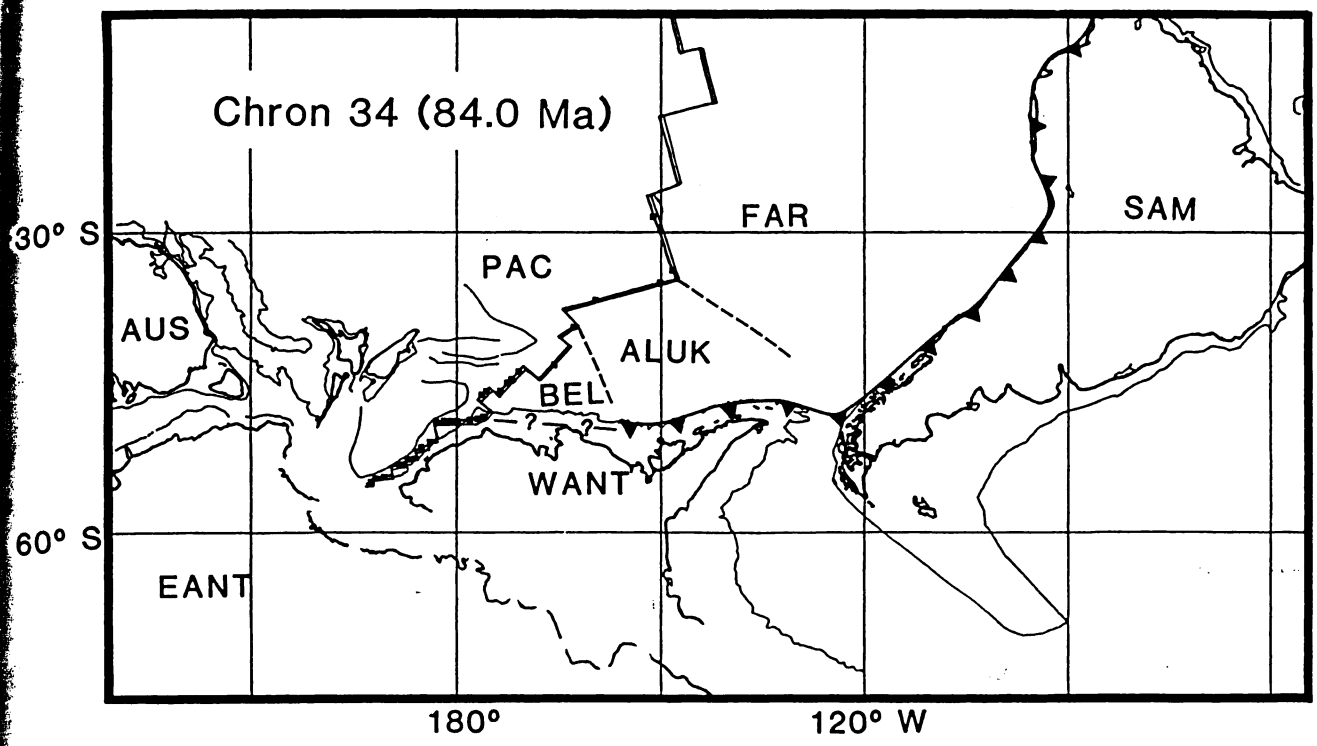

Fig. 8. Tectonic reconstruction for Chron 34 (84.0 Ma). In the southwest Pacific, spreading began between the Campbell Plateau and the Chatham Rise and Marie Byrd Land. Spreading was also occurring along the Pacific-Bellingshausen and Pacific-Aluk plate boundaries. Bounty Trough opened, which rifted the Chatham Rise away from the Campbell Plateau. A double line indicates the active spreading centers; squares are anomaly identifications on the Pacific plate; circles are anomaly identifications on the Antarctic plate; triangles are anomaly identifications on the Farallon (Nazca) plate. The relative positions of East Antarctica and Weddellia were obtained only by deriving the relative positions of the two pieces of New Zealand.

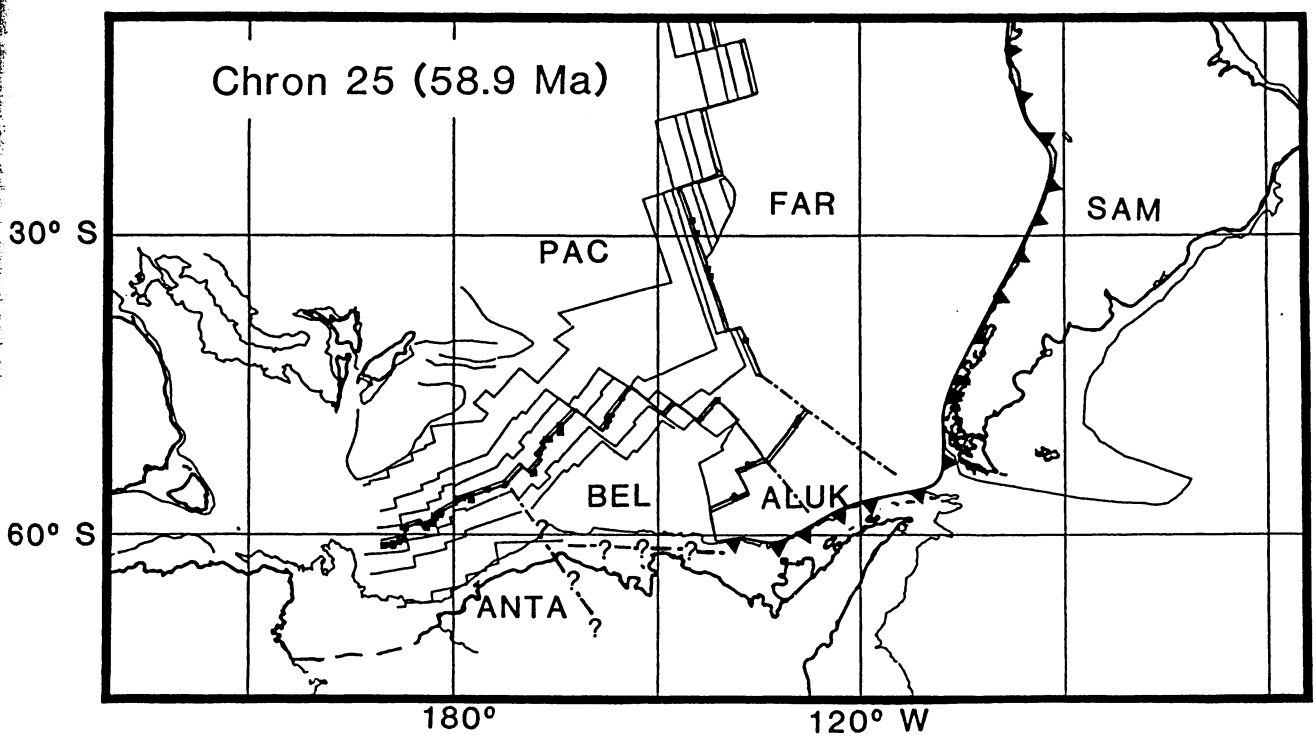

Fig. 9. Tectonic reconstruction for Chron 25 (58.9 Ma). The dual spreading centers in the southeast Pacific continued to separate. Motion in the Ross Sea also continued, but the Tasman Sea has reached its maximum opening at Chron 25. Apparent separation between the two parts of New Zealand is probably due to the accumulated error of the Pacific-Antarctica, Antarctica-Australia and Australia-Lord Howe Rise plate circuit. Symbols as in Figure 8.

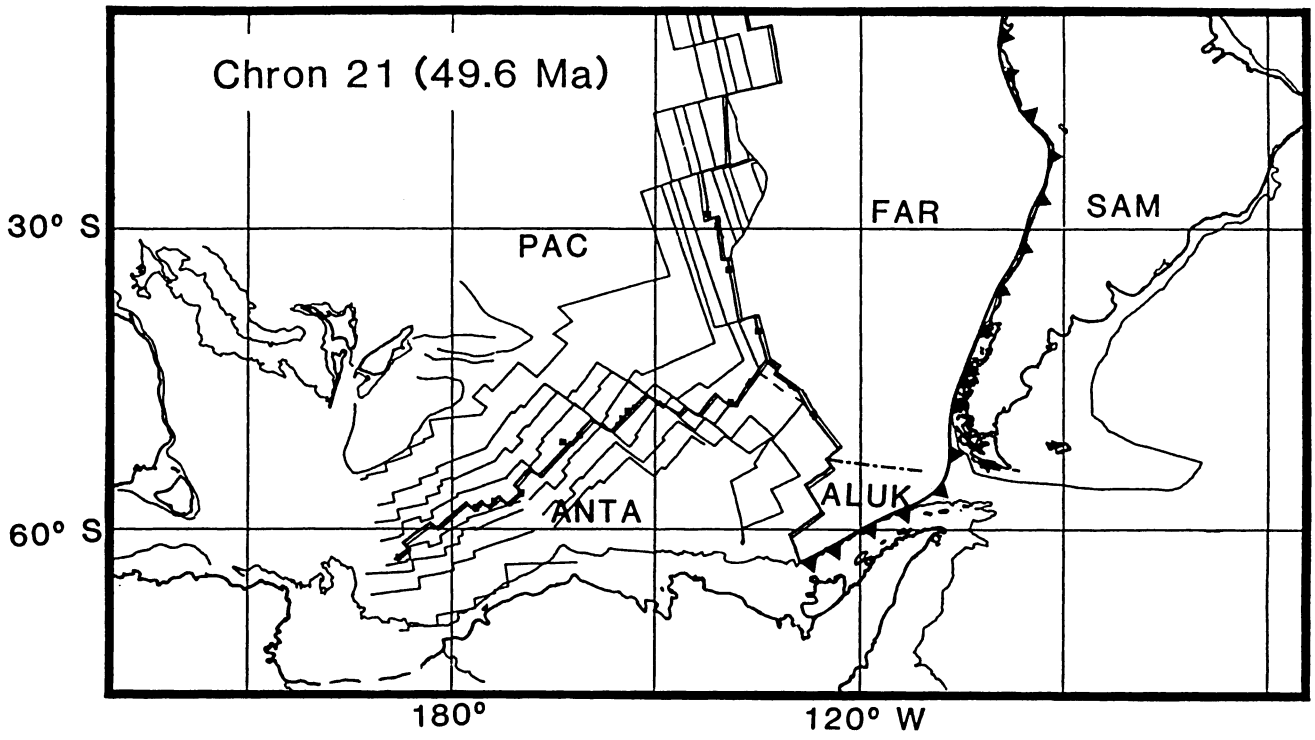

Fig. 10. Tectonic reconstruction for Chron 21 (49.6 Ma). Major changes occurred in the plate configuration in the South Pacific. The Pacific-Antarctic Rise began spreading about the same pole from the Macquarie Ridge to the Pacific-Antarctic-Farallon triple junction. Motion between Marie Byrd Land and the Bellingshausen plate ceased. The Pacific-Antarctic Rise had broken through the older crust on the Pacific-Aluk spreading center and transferred a piece of northward aging crust created at the old spreading center to the Antarctic plate [*Cande et al.*, 1982]. The Farallon plate began to move in a more northerly direction relative to the Antarctic plate, creating anomaly 23 to anomaly 21 to the north of the Humboldt Trough. A segment of the Antarctic-Aluk spreading center collided with the Antarctic margin in the vicinity of Alexander Island. Symbols as in Figure 8.

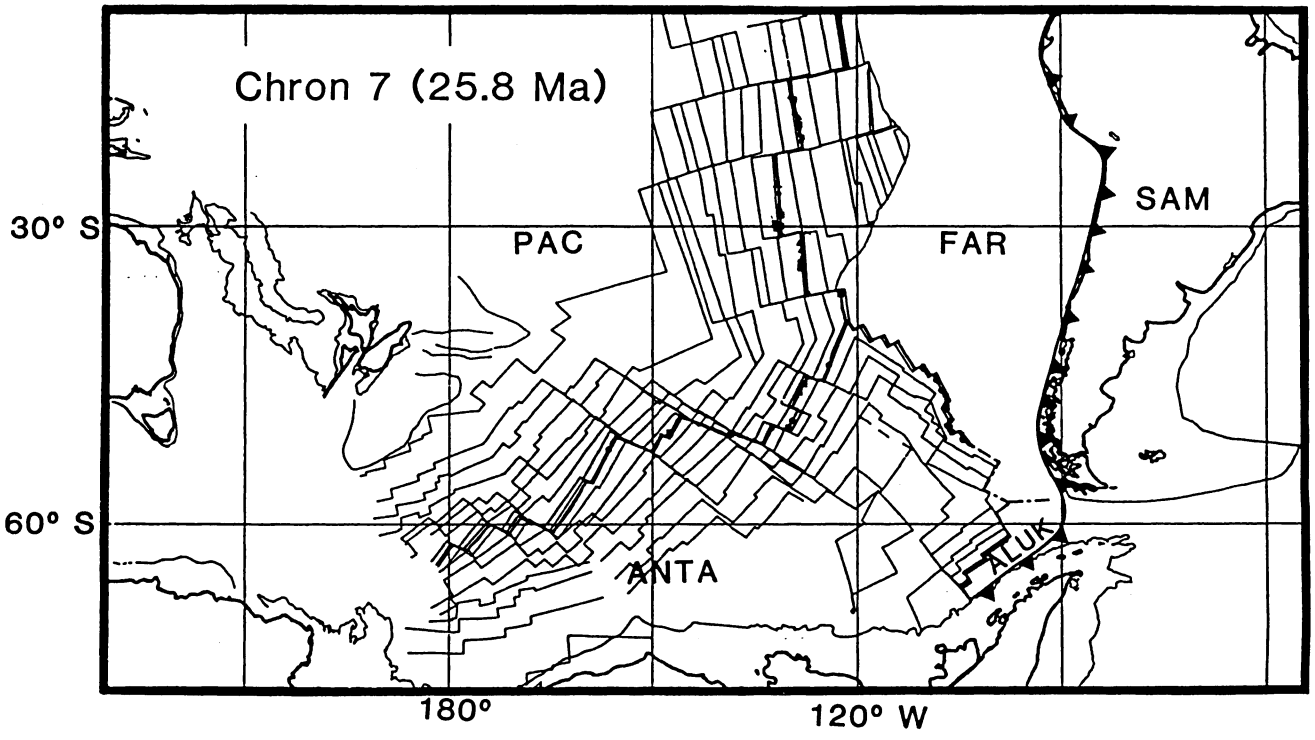

Fig. 11. Tectonic reconstruction for Chron 7 (25.8 Ma). Antarctic-Farallon spreading center was gradually reorienting itself to a more northerly direction. Symbols as in Figure 8.

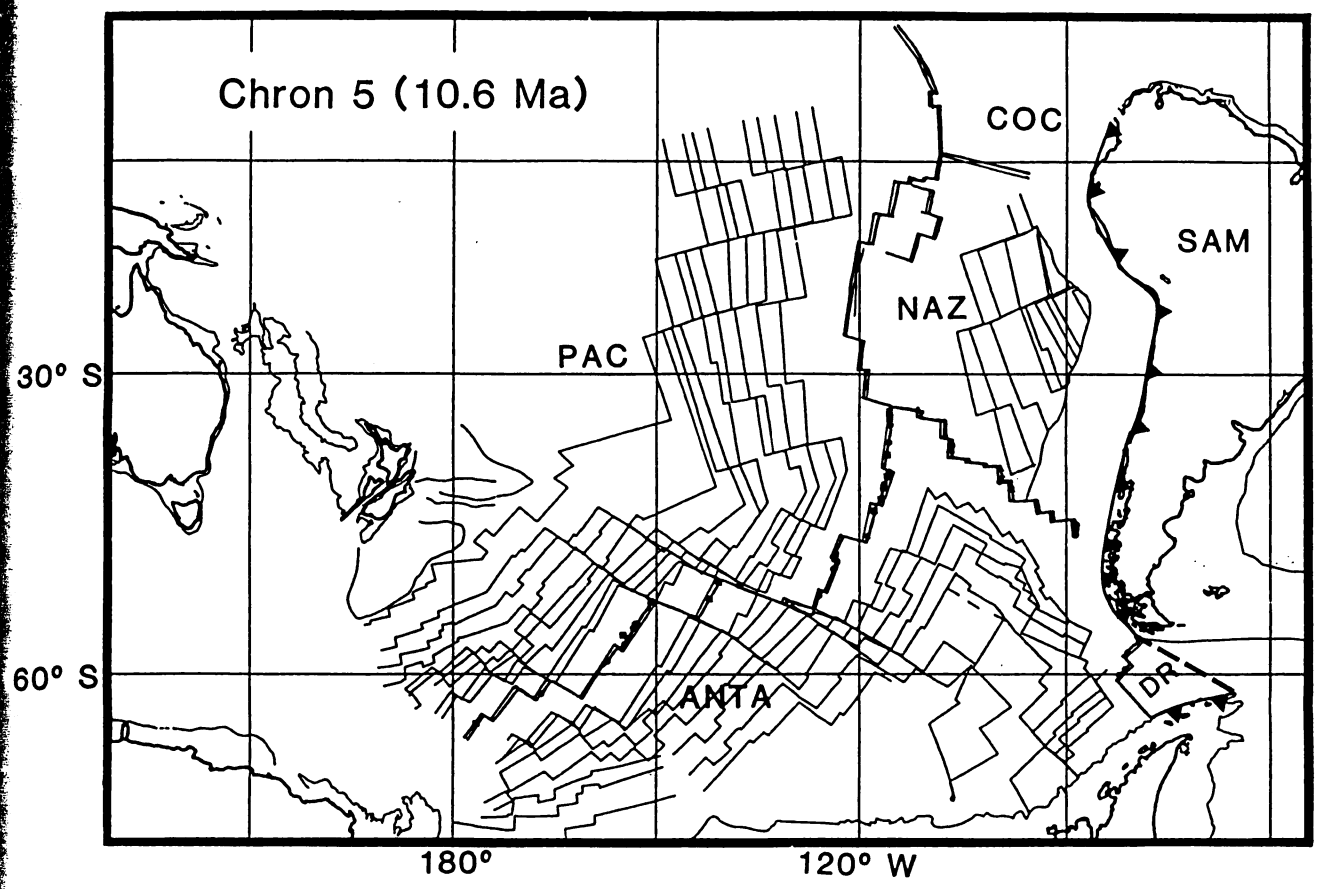

Fig. 12. Tectonic reconstruction for Chron 5 (10.6 Ma). The Farallon plate broke into two plates, the Cocos and the Nazca plates and rifting initiated along the Galapagos Spreading Center. The Pacific-Farallon spreading center (now Pacific-Nazca and Pacific-Cocos) was reoriented from a northwesterly to a northeasterly orientation. This new East Pacific Rise was spreading along a dual spreading center, along both the East Pacific Rise and the Galapagos Rise. The Chile Rise had been reoriented to almost north-south spreading. Another ridge-trench collision along the Antarctic margin between the Tula and Hero Fracture Zones had occurred. Movement began on the Alpine Fault in New Zealand. Symbols as in Figure 8.

Pacific-Antarctic-Farallon triple junction, which we show as a RRR type, moved rapidly 600 km to the northwest [*Cande et al.*, 1982]. The old Pacific-Aluk spreading center became the Antarctic-Aluk spreading center when the Pacific-Antarctic spreading center cut through to the Farallon plate at the time of anomaly 21.

Between Chron 7 (Figure 11) and Chron 5 (Figure 12), major changes in plate motion took place in the South Pacific. The Farallon plate broke into two plates: the Cocos plate to the north and the Nazca plate to the south [*Herron and Heirtzler*, 1987; *Raff*, 1968], with the spreading direction changing from a northeasterly to a northwesterly direction. For a short period after this plate reorganization, spreading on the Pacific-Nazca boundary occurred on both the East Pacific Rise and the Galapagos Rise along a dual spreading center [*Herron*, 1972; *Anderson and Sclater*, 1982; *Mammerickx et al.*, 1980]. Seafloor spreading on the Galapagos Rise stopped at about Chron 4 (6.5 Ma). At the same time, the spreading rate on the Pacific-Antarctic Rise increased from about 30 mm/yr to about 50 mm/yr on the northern part of the ridge. The Chile Rise also underwent a major change in orientation from a northwesterly orientation to a more north-south orientation [*Cande et al.*, 1982]. The Pacific-Antarctic-Nazca triple junction changed from a RRR to a RFF type.

During the past 5 m.y., the Pacific region has been relatively stable. The most noticeable changes have been the development of the Easter microplate at about the time of anomaly 2 [*Handschumacher et al.*, 1981], the development of the Juan Fernandez microplate at the Pacific-Nazca-Antarctic triple junction [*Anderson-Fontana et al.*, 1986], and the abandonment of the Mathematician Ridge at about the time of anomaly 3 [*Mammerickx et al.*, 1988].

DISCUSSION AND CONCLUSIONS

Our study demonstrates that the use of geoid data, in conjunction with shipboard data, improves our ability to define the past positions of plates relative to each other and can help us understand in more detail the way that plates move with respect to each other. This is especially important where large regions are difficult to access by ship, such as the South Pacific. While gridded geoid and gravity maps derived from satellite altimetry [*Haxby*, 1987] provide an overview of the tectonic fabric of the oceans, our presentation of the Geosat data as plots of slope of the geoid (vertical deflection) along satellite tracks have greater detail and accuracy which are better for quantitative research. Because the flow lines which we can trace in the Geosat data are

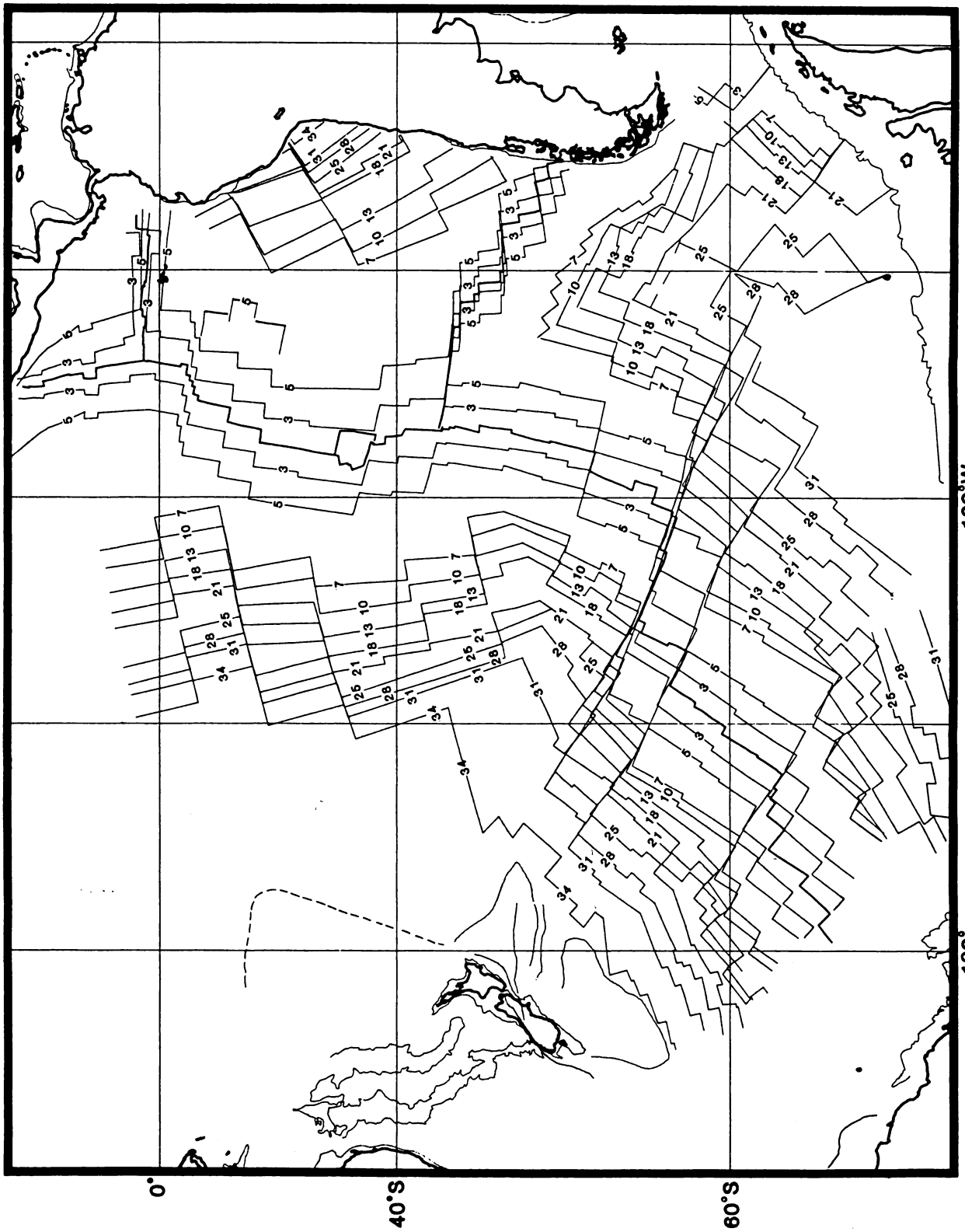

Fig 13. Present-day. Isochron chart of the South Pacific generated using the locations of the old spreading centers from our reconstructions.

well-correlated with bathymetric identifications of fracture zones, these lineations in the vertical deflection charts can be used for plate reconstructions just as bathymetric lineations have been used in the past. The satellite altimetry data represent an improvement over the bathymetric identifications because they are more uniformly sampled. Using our vertical deflection lineations along with bathymetric lineations and a compilation of published magnetic anomaly identifications and magnetic lineations, we have constructed a tectonic fabric map of the South Pacific region. We used the features on the tectonic fabric map to calculate paleogeographic reconstructions for the Cenozoic and Late Cretaceous.

The past positions of the spreading centers derived from the tectonic chart and our poles of reconstruction are compiled into an isochron chart of the South Pacific (Figure 13). The fracture zones along the ridges are drawn parallel to the lineations in the vertical deflection charts and to small circles about the stage poles and not as continuous features in the isochron chart. The poles of reconstruction for the Pacific-Antarctic and Pacific-Bellingshausen plate pairs are, in most cases, within the margin of error of the calculations of *Stock and Molnar* [1987]. A notable exception to this is the anomaly 18 pole of the Pacific-Bellingshausen plate pair. This might be explained by a paucity of data for anomaly 18 along the Pacific-Bellingshausen boundary.

There are several interesting features on the isochron chart. First, our study predicts that the oldest crust on the Nazca plate is older than anomaly 34 (84.0 Ma). Second, the age of the oldest crust on the Cocos plate is still uncertain. Third, we have been able to successfully model the changes in distance between the Heezen and Tharp fracture zones by examining the changes in relative motion between the Pacific and Antarctic plates. The fracture zones drawn according to the small circles generated from our stage poles indicate that at around Chron 10, the spreading on the Pacific-Antarctic Ridge became briefly more east-west oriented than it was before or after, and this caused the length of the ridge segment between the two fracture zones to decrease for a short period of time.

The deflection of the vertical chart has helped clarify and date the change in spreading direction along the Pacific-Antarctic spreading center. *Stock and Molnar* [1987] date the time of the change from separate Pacific-Bellingshausen and Pacific-Antarctic spreading centers to one ridge spreading about one pole at approximately Chron 18 (42.7 Ma). However, the change in geoid signal on the Pacific plate (south of the Campbell Plateau) from smooth (north) to numerous lineations (south) occurs just south of the anomaly 25 identifications of *Christoffel and Falconer* [1982] and *Stock and Molnar* [1987]. Vertical deflection lineations which represent fracture zone trends south of anomaly 25 are parallel to lineations further to the south on the Pacific plate. In addition, the picks and lineations of *Molnar et al.* [1975] allow us to use an orientation parallel to the younger trends between anomaly 21 and anomaly 18 because they are sparse and widely spaced.

The most remarkable change in plate configuration happened in the South Pacific at about Chron 21 when the Pacific-Antarctic spreading center jumped northward and trapped on the Antarctic plate a piece of northward aging crust created at the Pacific-Aluk spreading center. The vertical deflection chart gives evidence of this jump in the expression of the Henry Trough on the Pacific plate and the Hudson Trough on the Antarctic plate. In addition, the difference in spreading rate between the fast Pacific-Aluk spreading center and the slower Pacific-Antarctic spreading is expressed in the Geosat data. To the north of the Henry Trough, the lineations are sparse, reflecting the fast spreading rate (156 mm/yr) of the Pacific-Aluk boundary, whereas to the south, the lineations are abundant, reflecting the slower spreading rate (50 mm/yr) on the Pacific-Antarctic boundary.

The deflection of the vertical fabric also helps resolve the question of relative motion between a hypothesized North Pacific plate and a South Pacific plate proposed by *Gordon and Cox* [1980] and *Jurdy and Gordon* [1984]. From the Geosat data, it can be concluded that the Pacific and Farallon plates were spreading apart about one pole from at least the Mendocino Fracture Zone to the Pacific-Antarctic-Farallon triple junction from the end of the Cretaceous Magnetic Quiet Period to the time when the Farallon plate broke into the Nazca and Cocos plates. The fracture zones which cut crust of Chron 34 age to the present-day ridge appear to be parallel and continuous (Plate 3).

Our study has raised several questions about the South Pacific that need further study. The most important problem yet to be resolved is that the Galapagos Spreading Center cannot be reconstructed according to plate tectonic theory at this time. We feel that our reconstructions are very well constrained on the northern part of the EPR by the magnetic anomaly identifications of *Klitgord and Mammerickx* [1982] and by our interpretation of the lineations in the vertical deflection charts. The southern limb of the EPR is much less well constrained by magnetic anomaly identifications (Plate 2); however, with good poles of rotation for Nazca-Antarctic and Antarctic-Pacific, we can calculate poles for Pacific-Nazca rotation along the southern EPR. Using these poles for the northern and southern EPR, we are unable to reasonably model the motion between the Nazca and Cocos plates.

The southern EPR from the Pacific-Nazca-Cocos triple junction to the Pacific-Nazca-Antarctic triple junction needs to be restudied, and the magnetic anomalies should be carefully charted. Also, along the older northwesterly trending segment of the Pacific-Farallon spreading center north of 30°S, the magnetic anomaly lineations must be recharted. A possible method for doing this could be based upon extrapolating the identifications of *Cande et al.* [1982] northward and using the lineations in the vertical deflection charts as a guide for spreading direction.

In the south, the age and structure of the crust north of Marie Byrd Land remain a mystery. The calculations of *Stock and Molnar* [1987] indicate the existence of a plate boundary in this region. Since this area is covered year round with ice and lies south of the geoid satellite coverage area, it will be difficult to determine the age of this area of the Antarctic plate and to explore the conjugate of the only passive margin in the South Pacific region.

A history of the crust to the north and west of the anomaly 34 identifications of *Cande et al.* [1982] and west of the Tonga-Kermadec trench needs to be developed. Much of this area lies within the Cretaceous Magnetic Quiet Period; however, the morphology of the seafloor might yield clues to the history of this area.

Acknowledgments. This paper was originally written as a thesis by Catherine L. Mayes at the University of Texas at Austin under the supervision of John Sclater. We would thank Ian Dalziel, Christoph Heubeck, and Dale Sawyer for reviewing the paper. We would also like to thank Joann Stock for her careful and helpful review of the reconstructions and poles of rotation. This work was supported by the Shell Professorship granted to John Sclater, a Teaching Assistantship in the Department of Geological Sciences, and the Geology Foundation at the University of Texas at Austin; the Paleoceanographic Mapping Project, the Institute for Geophysics, and the NASA Geodynamics Program (NAG5-787).

REFERENCES

Anderson, R. N., and J. G. Sclater, Evolution of the East Pacific Rise, *Earth Planet. Sci. Lett.*, *14*, 433-441, 1972.

Anderson-Fontana, S., J. F. Engeln, P. Lundgren, R. L. Larson, and S. Stein, Tectonics and evolution of the Juan Fernandez microplate at the Pacific-Nazca-Antarctic triple junction, *J. Geophys. Res.*, *91*, 2005-2018, 1986.

Barker, P. F., The Cenozoic subduction history of the Pacific margin of the Antarctic Peninsula: Ridge crest-trench interactions, *J. Geol. Soc. London*, *139*, 787-801, 1982.

Berggren, W. A., D. V. Kent, J. J. Flynn, and J. A. Van Couvering, Cenozoic geochronology, *Geol. Soc. Am. Bull.*, *96*, 1407-1418, 1985.

Bonatti, E., C. G. A. Harrison, D. E. Fisher, J. Honnorez, J.-G. Schilling, J. J. Stipp, and M. Zentilli, Easter volcanic chain (southeast Pacific): A mantle hot line, *J. Geophys. Res.*, *82*, 2457-2478, 1977.

Burns, R. E., et al., Site 207, *Initial Rep. Deep Sea Drill. Proj.*, *21*, 197-269, 1973.

Cande, S. C., and R. B. Leslie, Late Cenozoic tectonics of the southern Chile Trench, *J. Geophys. Res.*, *91*, 471-496, 1986.

Cande, S. C., E. M. Herron, and B. R. Hall, The early Cenozoic history of the southeast Pacific, *Earth Planet. Sci. Lett.*, *57*, 63-74, 1982.

Cande, S. C., J. L. LaBrecque, and W. F. Haxby, Plate kinematics of the South Atlantic: Chron C34 to Present, *J. Geophys. Res.*, *93*, 13,479-13,492, 1988.

Cheney, R. E., B. C. Douglas, R. W. Agreen, L. L. Miller, D. L. Porter, and N. S. Doyle, Geosat altimeter geophysical data record user handbook, *NOAA Tech. Memo., NOS Ngs-46*, 32 pp., 1987.

Christoffel, D. A., and R. H. H. Falconer, Marine magnetic measurements in the southwest Pacific Ocean and the identification of new tectonic features, in *Antarctic Oceanology II: The Australian-New Zealand Sector, Antarct. Ser.*, vol. 19, edited by D. E. Hayes, pp. 197-209, AGU, Washington, D.C., 1972.

Craig, C. H., and D. T. Sandwell, The global distribution of seamounts from Seasat profiles, *J. Geophys. Res.*, *93*, 10,408-10,420, 1988.

Crook, K. A. W., and L. Belbin, The southwest Pacific area during the last 90 million years, *J. Geol. Soc. Aust.*, *25*, 23-40, 1978.

Dalziel, I. W. D., and D. H. Elliot, West Antarctica: Problem child of Gondwanaland, *Tectonics*, *1*, 3-19, 1982.

Drewry, D. J., and S. R. Jordan, "Bedrock surface of Antarctica", in *Antarctica: Glaciological and Geophysical Folio*, edited by D. J. Drewry, sheet 3, Scott Polar Research Institute, Cambridge, 1983.

Falconer, R. K. H., and M. Tharp, GEBCO panel 5.14, IHO/IOC/CHS, GEBCO-General bathymetric chart of the oceans, 5th ed., Int. Hydrogr. Organ./Intergovern. Oceanic Comm./Can. Hydrogr. Serv., Ottawa, Ont., 1984.

Gordon, R.G., and A. Cox, Paleomagnetic test of the early Tertiary plate circuit between the Pacific Basin plates and the Indian plate, *J. Geophys. Res.*, *85*, 6534-5646, 1980.

Grindley, G. W., and F. J. Davey, The reconstruction of New Zealand, Australia, and Antarctica, in *Antarctic Geoscience*, edited by C. Craddock, pp. 15-29, University of Wisconsin Press, Madison, 1982.

Grunow, A. M., D. V. Kent, and I. W. D. Dalziel, Mesozoic evolution of West Antarctica and the Weddell Sea Basin: New paleomagnetic constraints, *Earth Planet. Sci. Lett.*, *86*, 16-26, 1987.

Handschumacher, D. W., Post-Eocene plate tectonics of the Eastern Pacific, in *The Geophysics of the Pacific Ocean Basin and Its Margins*, *Geophys. Monogr. Ser.*, vol. 19, edited by G. H. Sutton et al., pp. 177-202, AGU, Washington, D.C., 1976.

Handschumacher, D. W., R. H. Pilger, Jr., J. A. Foreman, and J. F. Campbell, Structure and evolution of the Easter plate, *Mem., Geol. Soc. Am.*, *154*, 63-76, 1981.

Harland, W. B., A. Cox, P. G. Llewellyn, C. A. G., Pickton, A. G. Smith, and R. Walters, A Geologic Time Scale, Cambridge University Press, New York, 1982.

Hayes, D. E., and J. Ringis, Sea-floor spreading in the Tasman Sea, *Nature*, 454-458, 1973.

Haxby, W. F., Gravity field of the world's oceans, *NOAA Rep. MGG-3*, 1987.

Herron, E. M., Sea-floor spreading and the Cenozoic history of the east-central Pacific, *Geol. Soc. Am. Bull.*, *83*, 1671-1692, 1972.

Herron, E. M., and J. R. Heirtzler, Sea-floor spreading near the Galapagos, *Science*, *158*, 775-780, 1967.

Herron, E. M., and B. E. Tucholke, Sea-floor magnetic patterns and basement structure in the southeastern Pacific, *Initial Rep. Deep Sea Drill. Proj.*, *35*, 263-278, 1976.

Hey, R., Tectonic evolution of the Cocos-Nazca spreading center, *Geol. Soc. Am. Bull.*, *88*, 1404-1420, 1977.

Johnson, G. L., and J.-R. Vanney, GEBCO Panel 5.18, IHO/IOC/CHS, GEBCO-General bathymetric chart of the oceans, 5th ed., Int. Hydrogr. Organ./Intergovern. Oceanic Comm./Can. Hydrogr. Serv., Ottawa, Ont., 1984.

Jurdy, D. M., and R. G. Gordon, Global plate motions relative to the hot spots 64 to 56 Ma, *J. Geophys. Res.*, *89*, 9927-9936, 1984.

Kamp, P. J. J., Late Cretaceous-Cenozoic tectonic development of the southwest Pacific region, *Tectonophysics*, *121*, 225-251, 1986.

Karig, D. E., Ridges and basins of the Tonga-Kermadec Island Arc system, *J. Geophys. Res.*, *75*, 239-254, 1970.

Kent, D. V., and F. M. A. Gradstein, Cretaceous and Jurassic geochronology, *Geol. Soc. Am. Bull.*, *96*, 1419-1427, 1985.

Klitgord, K. D., and P. Lonsdale, Structure and tectonic history of the eastern Panama Basin, *Geol. Soc. Am. Bull.*, *89*, 981-999, 1978.

Klitgord, K. D., and J. Mammerickx, Northern East Pacific Rise: Magnetic anomaly and bathymetric framework, *J. Geophys. Res.*, 6725-6750, 1982.

Klitgord, K. D., and H. Schouten, Plate kinematics of the central Atlantic, *The Geology of North America, vol. M, The Western North Atlantic Region*, edited by P. R. Vogt and B. E. Tucholke, pp. 351-378, Geological Society of America, Boulder, Colo., 1986.

Lanphere, M., and G. B. Dalrymple, K-Ar ages of basalts from DSDP leg 33: Sites 315 (Line Islands) and 317 (Manihiki Plateau), *Initial Rep. Deep Sea Drill. Proj.*, *33*, 649-654, 1976.

Larson, R. L., Late Jurassic and Early Cretaceous evolution of the western central Pacific Ocean, *J. Geomagn. Geoelectr.*, *28*, 219-236, 1976.

Lawver, L. A., J. G. Sclater, and L. Meinke, Mesozoic and Cenozoic reconstructions of the South Atlantic, *Tectonophysics*, *114*, 233-254, 1985.

Lonsdale, P., Geography and history of the Louisville hotspot chain in the southwest Pacific, *J. Geophys. Res.*, *93*, 3078-3104, 1988.

MacArthur, J. L., P. C. Marsh, Jr., and J. G. Wall, The Geosat radar altimeter, *APL Tech. Dig.*, *8*, 176-181, 1987.

Mammerickx, J., Depth anomalies in the Pacific: Active, fossil and precursor, *Earth Planet. Sci. Lett.*, *53*, 147-157, 1981.

Mammerickx, J., and D. T. Sandwell, Rifting of old oceanic lithosphere, *J. Geophys. Res.*, *92*, 1975-1988, 1986.

Mammerickx, J., and S. M. Smith, GEBCO panel 5.7, IHO/IOC/CHS, GEBCO-General bathymetric chart of the oceans, 5th ed., Int. Hydrogr. Organ./Intergovern. Oceanic Comm./Can. Hydrogr. Ser., Ottawa, Ont., 1984*a*.

Mammerickx, J., and S. M. Smith, GEBCO panel 5.11, IHO/IOC/CHS, GEBCO-General bathymetric chart of the oceans, 5th ed., Int. Hydrogr. Organ./Intergovern. Oceanic Comm./Can. Hydrogr. Ser., Ottawa, Ont., 1984*b*.

Mammerickx, J., E. M. Herron, and L. Dorman, Evidence for two fossil spreading ridges in the southeast Pacific, *Geol. Soc. Am. Bull.*, *91*, 263-271, 1980.

Mammerickx, J., I. L. Taylor, and S. Cande, GEBCO panel 5.15, IHO/IOC/CHS, GEBCO-General bathymetric chart of the oceans, 5th ed., Int. Hydrogr. Organ./Intergovern. Oceanic Comm./Can. Hydrogr. Ser., Ottawa, Ont., 1984.

Mammerickx, J., D. F. Naar, and R. L. Tyce, The Mathematician paleoplate, *J. Geophys. Res.*, *93*, 3025-3040, 1988.

Marsh, J. G., and T. V. Martin, The Seasat altimeter mean sea surface model, *J. Geophys. Res.*, *87*, 3269-3280, 1982.

McConathy, D. R., and J. J. Kilgus, The Navy Geosat Mission: An overview, *APL Tech. Dig.*, *8*, 170-175, 1987.

Menard, H. W., The East Pacific Rise, *Science*, *132*, 1737-1746, 1960.

Menard, H. W., Fracture zones and offsets of the East Pacific Rise, *J. Geophys. Res.*, *71*, 682-685, 1966.

Molnar, P., T. Atwater, J. Mammerickx, and S. M. Smith, Magnetic anomalies, bathymetry and the tectonic evolution of the South Pacific since the Late Cretaceous, *Geophys. J. R. Astron. Soc.*, *40*, 383-420, 1975.

Monahan, D., R. K. H. Falconer, and M. Tharp, GEBCO panel 5.10, IHO/IOC/CHS, GEBCO-General bathymetric chart of the oceans, 5th ed., Int. Hydrogr. Organ./Intergovern. Oceanic Comm./Can. Hydrogr. Ser., Ottawa, Ont., 1984.

Okal, E. A., and A. Cazenave, A model for the plate tectonic evolution of the east-central Pacific based on Seasat investigations, *Earth Planet. Sci. Lett.*, *72*, 99-116, 1985.

Palmer, A. R., The decade of North American geology 1983 geologic time scale, *Geology*, *11*, 503-504, 1983.

Pardo-Casas, F., and P. Molnar, Relative motion of the Nazca (Farallon)

and South American plates since Late Cretaceous time, *Tectonics*, *6*, 215-232, 1987.

Patriat, P. L., Evolution du systme de dorsales de l'Ocean Indien, these doctorat d'etat, Univ. Pierre et Marie Curie, Paris, 1983.

Pitman, W. C., III, E. M. Herron, and J. R. Heirtzler, Magnetic anomalies in the Pacific and sea floor spreading, *J. Geophys. Res.*, *73*, 2069-2085, 1968.

Raff, A. D., Sea-floor spreading: another rift, *J. Geophys. Res.*, *73*, 3699-3705, 1968.

Rosa, J. W. C., and P. Molnar, Uncertainties in reconstructions of the Pacific, Farallon, Vancouver and Kula plates and constraints on the rigidity of the Pacific and Farallon (and Vancouver) plates between 72 and 35 Ma, *J. Geophys. Res.*, *93*, 2997-3008, 1988.

Ross, M. I., and C. R. Scotese, Hierarchical tectonic analysis of the Gulf of Mexico and Caribbean Region, *Tectonophysics*, *155*, 138-168, 1988.

Royer, J.-Y., and D. S. Sandwell, Evolution of the Eastern Indian Ocean since the late Cretaceous: Contraints from Geosat altimetry, *J. Geophys. Res.*, *94*, 13,755-13,782, 1989.

Sailor, R. V., and E. A. Okal, Applications of Seasat altimeter data in seismotectonic studies of the south central Pacific, *J. Geophys. Res.*, *88*, 1572-1580, 1983.

Sandwell, D. T., and D. C. McAdoo, Marine gravity of the Southern Ocean and Antarctic margin from Geosat, *J. Geophys. Res.*, *93*, 10,389-10,396, 1988.

Sandwell, D. T., and G. Schubert, Geoid and height-age relation from Seasat altimeter profiles across the Mendocino Fracture Zone, *J. Geophys. Res.*, *87*, 3949-3958, 1982.

Sclater, J. G., R. N. Anderson, and M. L. Bell, Elevation of ridges and evolution of the central eastern Pacific, *J. Geophys. Res.*, *76*, 7888-7915, 1971.

Scotese, C. R., L. M. Gahagan, and R. L. Larson, Plate tectonic reconstructions of the Cretaceous and Cenozoic ocean basins, *Tectonophysics*, *155*, 27-48, 1988.

Shaw, P. R., and S. C. Cande, Shape and amplitude analysis of small-offset fracture zone geoid signals, *Eos Trans. AGU*, *68*, 1462, 1987.

Stock, J., and P. Molnar, Uncertainties in the relative positions of the Australia, Antarctica, Lord Howe, and Pacific plates since the Late Cretaceous, *J. Geophys. Res.*, *87*, 4697-4714, 1982.

Stock, J., and P. Molnar, Revised history of early Tertiary plate motion in the south-west Pacific, *Nature*, *325*, 495-499, 1987.

Tapley, B. D., G. H. Born, and M. E. Parke, The Seasat altimeter data and its accuracy assessment, *J. Geophys. Res.*, *87*, 3179-3188, 1982.

Watts, A. B., J. K. Weissel, R. A. Duncan, and R. L. Larson, Origin of the Louisville Ridge and its relationship to the Eltanin Fracture Zone system, *J. Geophys. Res.*, *93*, 3051-3077, 1988.

Weissel, J. K., and D. E. Hayes, Evolution of the Tasman Sea reappraised, *Earth Planet. Sci. Lett.*, *36*, 77-84, 1977.

L. A. Lawver, Institute for Geophysics, University of Texas at Austin, 8701 Mopac Blvd., Austin, TX 78759.

C. L. Mayes, Department of Geological Sciences, P.O. Box 7456, University of Texas at Austin, Austin, TX 78713-7456.

D. T. Sandwell, Geologic Research Division, Scripps Institution of Oceanography, A020, La Jolla, CA 92093.

(Received May 18, 1988;
revised August 15, 1989;
accepted August 16, 1989.)